Sixty years of research on ship rudders
Effects of design choices on rudder performance

Liu, Jialun; Hekkenberg, Robert

DOI
10.1080/17445302.2016.1178205

Publication date
2017

Document Version
Accepted author manuscript

Published in
Ships and Offshore Structures

Sixty years of research on ship rudders: Effects of design choices on rudder performance

Jialun Liu*, Robert Hekkenberg

Delft University of Technology, Mekelweg 2, 2628 CD, Delft, The Netherlands

Abstract

Rudders are primary steering devices for merchant ships. The main purpose of using rudders is to generate forces for course-keeping and manoeuvring. In exceptional cases, rudders are also used for emergency stopping and roll stabilisation. Furthermore, rudders affect propeller thrust efficiency and total ship resistance. Therefore, rudders are important to navigation safety and transport efficiency. The performance of rudders depends on the rudder hydrodynamic characteristics, which are affected by the design choices. Scholarly articles concerning the design of rudders date back more than 60 years. Moreover, a lot of knowledge fragments of rudders exist in literature where ship manoeuvrability and fuel consumption are discussed. It is worthwhile to gather this information not only for researchers to advance the state-of-the-art development but also for designers to make proper choices. To have a contemporary vision of the rudders, this paper presents a consolidated review of design impacts on rudder performance in ship manoeuvrability, fuel consumption, and cavitation. The discussed design choices are rudder working conditions (Reynolds numbers and angles of attack), profiles (sectional shapes), properties (area, thickness, span, chord, and rudder aspect ratios), types (the position of the stock and the structural rudder-hull connection), and interactions (among the hull, the propeller, and the rudder). Further research is suggested on high-lift rudder profiles, multiple-rudder configurations and interactions among the hull, the propeller, and the rudder. Recommendations for industry practices in the selection of the rudder design choices are also given.

Keywords: rudder profiles, rudder properties, rudder types, hull-propeller-rudder interactions, rudder performance, ship manoeuvrability

Nomenclature

Abbreviations

CFD Computational Fluid Dynamics

*Corresponding author.
Email address: J.Liu@tudelft.nl (Jialun Liu)

PRS	Propeller-rudder systems	
Re	Reynolds number	

Greek Symbols

α	Angle of attack	(rad)
α_0	Incidence for zero lift	(rad)
α_R	Effective rudder angle	(rad)
α_{stall}	Stall angle	(rad)
β	Ship drift angle	(rad)
β_R	Drift angle at the position of the rudder	(rad)
δ	Rudder angle relative to the ship centreline	(rad)
γ_R	Flow straightening factor	(−)
λ	Scale factor	(−)
Λ_E	Rudder effective aspect ratio, $\Lambda_E = k_\Lambda \Lambda_G$	(−)
Λ_G	Rudder geometric aspect ratio, $\Lambda_G = B_R/C_R$	(−)
μ	Water dynamic viscosity	($\mathrm{N\,s\,m^{-2}}$)
ρ	Water density	($\mathrm{kg\,m^{-3}}$)

Roman Symbols

a_H	Rudder force increase factor	(−)
A_m	Ship midship section area	($\mathrm{m^2}$)
A_R	Rudder area	($\mathrm{m^2}$)
B	Ship beam	(m)
B_R	Rudder span	(m)
C_B	Ship block coefficient	(−)

C_D	Drag coefficient	(−)
C_L	Lift coefficient	(−)
C_N	Normal force coefficient	(−)
C_R	Rudder chord length	(m)
C_T	Tangential force coefficient	(−)
C_{L_α}	Lift curve slope, $C_{L_\alpha} = dC_L/d\alpha$	(−)
$C_{L_{max}}$	Maximum lift coefficient	(−)
C_{YR_α}	Gradient of the rudder side force coefficient	(−)
C_{YR}	Rudder side force coefficient	(−)
D_P	Propeller diameter	(m)
D_R	Rudder drag force in the direction of the inflow	(N)
J_P	Propeller advance ratio	(−)
k_Λ	Ratio of the effective aspect ratio to the geometric aspect ratio, $k_\Lambda = \Lambda_E/\Lambda_G$	(−)
L_R	Rudder lift force perpendicular to the inflow direction	(N)
L_{pp}	Ship length between perpendiculars	(m)
n_P	Propeller revolution	(s^{-1})
N_R	Rudder normal force perpendicular to the rudder chord line	(N)
R_R	Resultant rudder force, $R_R = \sqrt{(N_R^2 + T_R^2)} = \sqrt{(L_R^2 + D_R^2)}$	(N)
T	Ship draught	(m)
T_R	Rudder tangential force in the direction of the rudder chord line	(N)
V_R	Rudder inflow speed	($m\,s^{-1}$)
x_{PR}	Longitudinal propeller-rudder separation	(m)
Y_R	Rudder induced side manoeuvring force	(newton)

y_{PR}	Lateral propeller-rudder separation	(m)
z_{PR}	Vertical propeller-rudder separation	(m)

Subscripts

E	Effective
F	Full-scale
G	Geometry
M	Model-scale

1. Introduction

Rudders are primarily applied on conventional ships for course keeping and manoeuvring. They are also used alone or with fins for roll stabilisation (Van Amerongen et al., 1990; Van Amerongen, 1991; Sharif et al., 1995, 1996; Perez, 2005; Surendran and Kiran, 2006, 2007; Lee et al., 2011; Ren et al., 2014). In over 60 years of research on ship rudders, only a limited number of fundamental studies have been published (Whicker and Fehlner, 1958; Thieme, 1962; Brix, 1993; Molland and Turnock, 2007). These studies provided valuable insights into the relationship of rudder design and rudder performance. However, it should be noted that previous studies of rudders in the open literature were mainly carried out for single NACA rudder cases, excluding the propeller and hull influences. To the best of authors' knowledge, impacts of the rudder design on ship manoeuvrability and fuel consumption have not been given great attention by the researchers in the past.

Initially, research on rudders is based on physical experiments in wind tunnels, towing tanks, or cavitation tunnels. However, these experiments have certain drawbacks, such as time and money consuming, limited model sizes, constrained Reynolds numbers, and influences of test equipment. With the rapid development of Computational Fluids Dynamics (CFD) methods, numerical analysis becomes possible. Even though CFD methods have numerical uncertainties, lack of validation data, and may also cost a lot of time and money, they still provide new opportunities for research on the rudder design. With the evolution of experiment techniques, the rudder design has been changing slowly. Therefore, the objective of this study is to gather information for researchers as well as designers to perform further developments and make proper choices.

This paper presents literature on the rudder design choices in five aspects: working conditions (Reynolds numbers and angles of attack), profiles (sectional shapes), properties (area, thickness, span, chord, and rudder aspect ratios), rudder types (the position of the stock and the structural rudder-hull connection), and interactions (among the hull, the

propeller, and the rudder). These design choices determine the amount and the direction of the rudder forces, resulting in different rudder performance. To avoid ambiguity, the rudder forces discussed in this paper, i.e. lift (L_R), drag (D_R), normal force (N_R), tangential force (T_R), and resultant force (R_R) are illustrated in Figure 1.

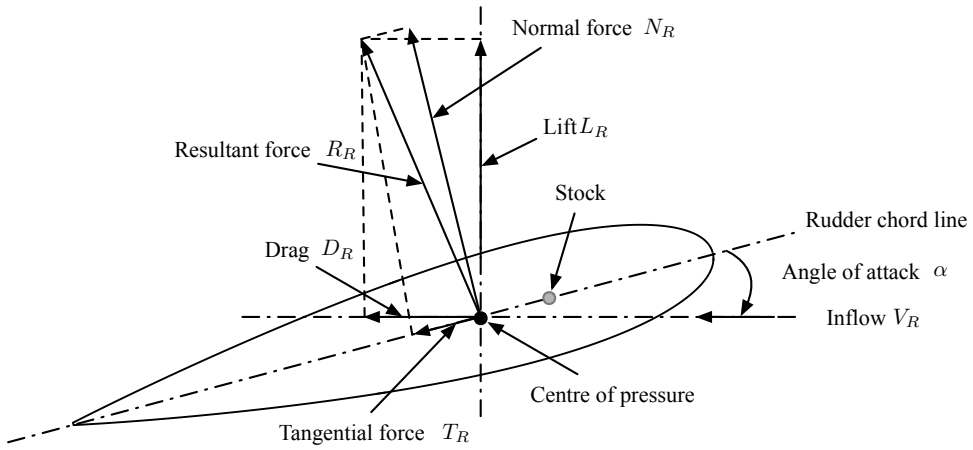

Figure 1: Rudder induced forces. Adapted from Molland and Turnock (2007, p. 73)

Lift is mainly generated by the pressure difference between the two surfaces. It is the component of the resultant force that acts perpendicular to the inflow direction. Lift nearly increases as a linear function of the angle of attack at the rate of $C_{L_\alpha} = dC_L/d\alpha$ (so-called lift curve slope) before the stall angle. The stall angle (α_{stall}) is the critical angle of attack at which maximum lift occurs. Normally, stall angles of rudders in open water are in the range of 15° to 20° and the practical stall angles in the propeller slipstream are in the range of 30° to 40°. In astern conditions, C_{L_α} reduces to 75 % to 85 % of the ahead condition, α_{stall} decreases by 5° to 10°, and C_{Lmax} is about 45 % to 75 % of the ahead case (Molland and Turnock, 2007, p. 99).

Drag is the rudder force component along the incidence flow direction, which consists of skin friction drag and form drag. Drag roughly increases parabolically with the angle of attack. The friction drag is caused by the frictional shear stress and determined by the size of the wetted surface. The form drag, also known as viscous pressure drag or pressure drag, primarily depends on the shape of the rudder. The friction drag is almost the same for rudders with the same wetted area while the form drag is relatively small. Thus, a streamlined profile may have smaller total drag than a blunt profile. At a Re of 2.4×10^5, Reichel (2009) concluded that under small rudder angles (up to 5°) almost all the tested six types of rudders with the same lateral area but different profiles and constructions have the same drag coefficients.

Routinely, non-dimensional coefficients are used to compare the rudder hydrodynamic performance with various design choices. Two main hydrodynamic characteristics are the lift coefficient (C_L) and the drag coefficient (C_D) based

on which the stall angle (α_{stall}), the maximum lift coefficient (C_{Lmax}), the normal force coefficient (C_N), the tangential force coefficient (C_T), and the lift to drag ratio (C_L/C_D) are identified. These parameters are non-dimensionalised and calculated as follows:

$$\begin{aligned} C_L &= L_R/(0.5\rho V_R^2 A_R) \\ C_D &= D_R/(0.5\rho V_R^2 A_R) \\ C_N &= C_L \cos\alpha + C_D \sin\alpha \\ C_T &= C_D \cos\alpha - C_L \sin\alpha, \end{aligned} \tag{1}$$

where ρ is water density, α is the angle of attack, V_R is the rudder inflow speed, A_R is the rudder area. Whicker and Fehlner (1958), Abbott and Von Doenhoff (1959), Thieme (1965), and Molland and Turnock (2007) provide further information about these coefficients.

In this paper, the rudder performance is evaluated in ship manoeuvrability, fuel consumption, and rudder cavitation. Additionally, the rudder effectiveness depends on the amount of the rudder induced side force (Y_R) for manoeuvring while the rudder efficiency relates to the lift to drag ratio. Rudders should first be effective for navigation safety and then be efficient for fuel consumption. More specifically, the rudder should be designed in such a way that sufficient manoeuvring force can be generated with minimal induced resistance. Furthermore, the design should also consider the rudder cavitation to reduce cost and time of maintenance.

This paper focuses on impacts of rudder design choices on rudder performance. State-of-the-art methods of experimental and numerical studies are presented. Challenges of achieving highly effective and efficient rudder design at the same time are found. Lack of knowledge in complex rudder configurations, such as high-lift rudder profiles and multiple-rudder interactions, is identified. Considering both navigation safety and fuel consumption, further research is suggested in the improvement of rudder effectiveness and efficiency. In Section. 2, literature that describes typical rudder working conditions of Reynolds numbers and angles of attack are presented. Influences of rudder types, profiles, and properties on rudder hydrodynamic characteristics are discussed in Section. 3, Section. 4, and Section. 5, respectively. Furthermore, Section. 6 introduces the interactions among the hull, the propeller, and the rudder. Section. 7 summaries evaluation of rudder performance in ship manoeuvrability, fuel consumption, and cavitation. Finally, Section. 8 draws conclusions.

2. Rudder working conditions

Rudder hydrodynamic characteristics indicate the rudder performance under specified conditions. The working conditions determine the actual amount and direction of forces induced by the rudder. This section presents the main operational conditions, i.e. Reynolds numbers (Re) and angles of attack (α).

2.1. Reynolds numbers

The Reynolds number (Re) is the ratio of momentum force to viscous force, expressing the relative importance of these two types of forces. Rudders may have different hydrodynamic characteristics at low Re (laminar flow) and high Re (turbulent flow). Based on the rudder chord length (C_R), full-scale Re of ship rudders range from about 5×10^5 for a small yacht up to about 1×10^8 for a large fast ship (Molland and Turnock, 2007, p. 34). For complete dynamic similarity of the flow conditions, Re has to be the same for both model-scale and full-scale in experimental and numerical tests. However, Re as high as 1×10^8 is commonly not achievable in contemporary physical test facilities.

For model tests, the rudder is scaled as the same as the ship. The relationship of model-scale and full-scale Re is as follows:

$$Re_F = \frac{\rho V_{R_F} C_{R_F}}{\mu} = \frac{\rho(\lambda^{0.5} V_{R_M})(\lambda C_{R_M})}{\mu} = \lambda^{1.5} Re_M, \tag{2}$$

where C_R is the rudder chord length, λ is the scale factor, and μ is the dynamic viscosity of water, subscripts F and M indicate full-scale and model-scale. In practice, Re_M is one order smaller than Re_F. The difference of Re violates the similarity of the rudder force in model-scale and full-scale manoeuvring motions. Accordingly, Ueno et al. (2014) and Ueno and Tsukada (2015) proposed corrections of rudder effectiveness and speed corrections for scaling model-scale results to realise the full-scale manoeuvring behaviours.

In general, an increase in Re leads to an increase in the lift coefficient and a decrease in the drag coefficient (Liu and Hekkenberg, 2016). Furthermore, the drag coefficient is more sensitive to the change of Re than the lift coefficient (Liu and Hekkenberg, 2016). Whicker and Fehlner (1958) indicated that Re influences are significant in the range of 1×10^6 to 3×10^6 and above 3×10^6 the impacts diminish. Ladson (1988) noted little variations of the coefficients above 6×10^6, which is also observed by Liu and Hekkenberg (2016) through series of CFD simulations of a NACA 0012 profile at Re in range of 4×10^6 to 1×10^7. Detailed information about impacts of Reynolds numbers on the rudder hydrodynamics was given by Loftin and Smith (1949).

To obtain insights into the rudder performance at high Re from actual low Re physical experiments, roughness strips are commonly attached near the model leading edge to generate turbulent flow instead of laminar flow. In practice, rudders nearly always work in fully turbulent flow due to the propeller rotation. CFD methods can study the full-scale open-water rudder hydrodynamics at high Re. Fach and Bertram (2007) reported the progress of CFD applications in simulations of rudder flows. However, the required simulation time and computation resource increase dramatically with the model size. To have a balance of computational cost and accurate results, it is favourable to test a model as large as possible at a sufficiently large Re above which lift and drag coefficients are slightly affected, for instance at Re of 6×10^6.

2.2. *Angle of attack*

The angle of attack (α) or the effective rudder angle (α_R) significantly affects the amount and direction of rudder forces. α_R is closely related to the rudder angle (δ) and the ship drift angle (β), which is commonly expressed as $\alpha_R = \delta - \beta$ (Yasukawa and Yoshimura, 2014). Greitsch (2008); Greitsch et al. (2009) applied operation profiles including the frequency distributions of rudder angles and ship speeds in rudder shape optimisation, cavitation risk analysis, and ship design. In addition, ships commonly sail with small rudder angles for course keeping. Brix (1993) indicated that the rotation caused by the propeller may induce an incidence of 10° to 15° to the rudder and a 10% increase in the rudder resistance. Therefore, it is beneficial to have the maximum lift to drag ratio and the minimal drag coefficient within this range to reduce the fuel consumption.

Records of rudder angles were taken on a 110 m long inland vessel by students supervised by the authors. Figure 2 presents histograms of applied rudder angles during the one journey from Antwerp, Belgium, to Vlaardingen, the Netherlands and the other journey from Vlaardingen, the Netherlands, to Hamm, Germany. It shows that the most frequently used rudder angles are in the range of −15° to 15°. This finding is quite similar to the frequency distribution published by Greitsch (2008) and Greitsch et al. (2009), which are rudder angles used by a ferry in the North Sea. It is worthwhile to mention that, in Figure 2, large rudder angles are also applied at relatively slow speed. These operations are typical for inland vessels but rarely seen on seagoing ships which have a customary maximum rudder angle of 35°. However, few studies have been made on the rudder performance at large angles of attack.

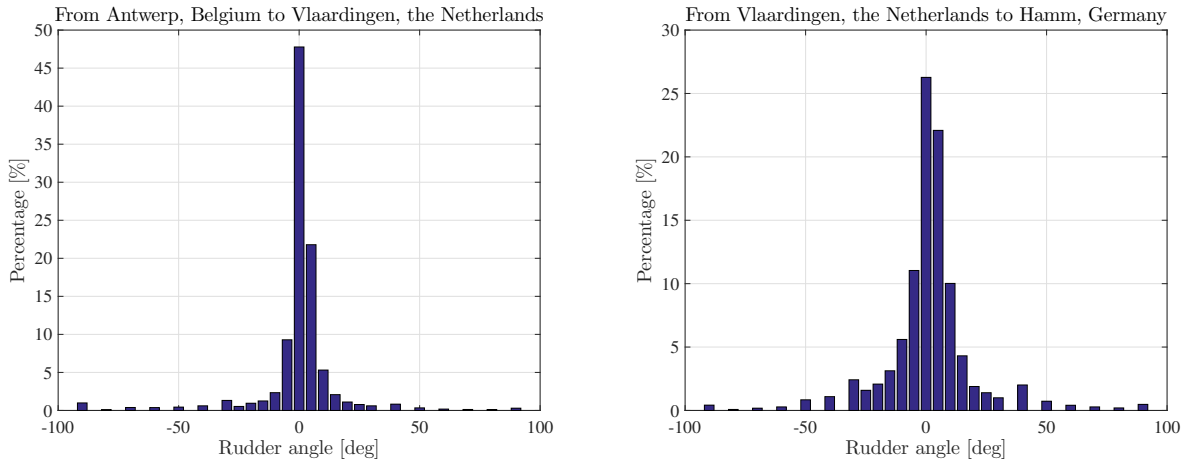

Figure 2: Frequency distributions of rudder angles for an inland vessel

2.3. *Recommendations for further research considering the working conditions*

As reviewed in the previous sections, the rudder performance depends on its working conditions, including, but not limited to, the Reynolds number and the angle of attack. Thus, ship operation profiles should be considered in

the process of the rudder design. A high Reynolds number can be achieved in tests by either enlarging the model size or increasing the inflow speed. Presently, model tests at high Reynolds number or full-scale ship tests may not be practical for primary studies due to the capacity of the test facilities or high expense. Another possible approach is the high-Reynolds-number CFD study. Considering the cost of high Reynolds number simulations with either model tests or CFD simulations, it is recommended to carry out tests at sufficiently high Reynolds numbers, for instance, a Reynolds number of 6×10^6, above which the rudder hydrodynamic characteristics may not be significantly affected by the change of the Reynolds number.

The main range of the applied rudder angles is $-35°$ to $35°$, which should be the main region of interest in the rudder hydrodynamics. Histograms of applied rudder angles and ship speeds like Figure 2 and results given by Greitsch (2008); Greitsch et al. (2009) are valuable for further studies on ship manoeuvring performance and fuel consumption. More operational data of different ships with various rudder configurations in inland waterways or open sea are needed. Furthermore, research works on the rudder performance for very slow moving ships, i.e. at Reynolds numbers lower than usual, with uncustomary large rudder angles are suggested, especially for inland vessels. In summary, further investigation and experimentation into the rudder hydrodynamic characteristics at various Reynolds number with practical operational profiles are recommended.

3. Rudder profiles

Rudder profiles are rudder sectional shapes. The profile is described by the rudder camber, the position of the maximum camber, the rudder thickness, the position of the maximum thickness, and the nose radius. Figure 3 illustrates the terminology to be used later in this paper. Various distributions of the camber and the thickness form different rudder series or families. Most of the existing rudder profiles are originally designed for aerofoils like the NACA series.

There are also profiles designed specially for ship rudders such as the IFS and HSVA series (Thieme, 1965). Other profiles including flat-plate, wedge-tail, fishtail, and flapped rudders are also discussed in this section. Figure 4 illustrates the typical rudder profiles which are discussed respectively in the following sections. Accordingly, different rudder profiles have different hydrodynamic characteristics leading to a different performance in ship manoeuvrability, fuel consumption, and rudder cavitation, which will be further discussed in Section. 7.

3.1. Flat plate

Flat-plate profiles are normally rectangles in two dimensions (square head in Figure 4). They are the simplest flow-deflecting devices to design, the easiest profiles to produce, and the cheapest rudders to buy. To reduce the form drag, flat-plate profiles may have semi-circle or triangular leading and trailing edges with faired tips (round

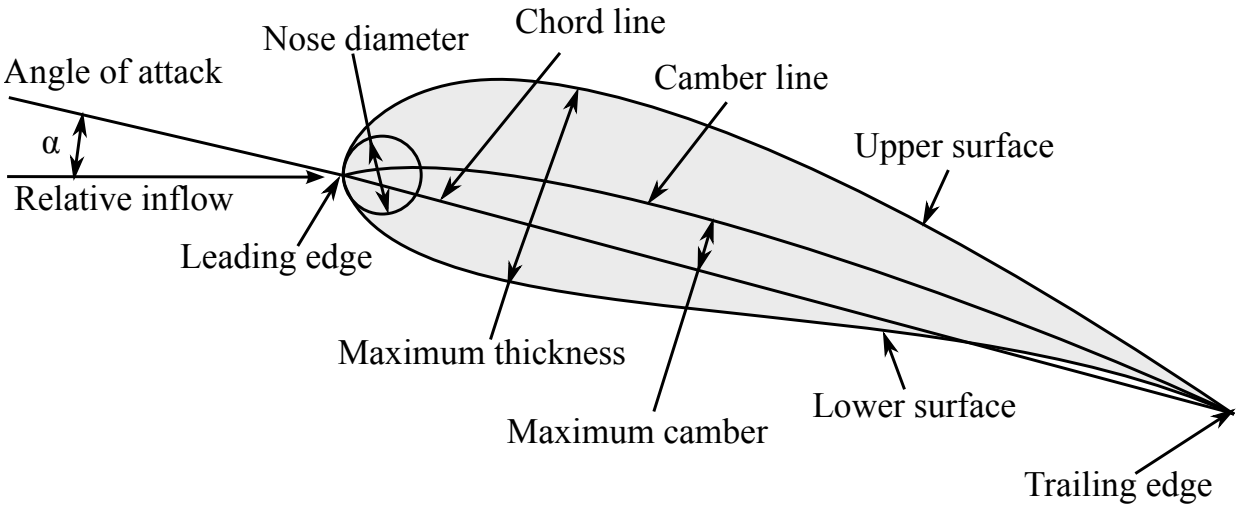

Figure 3: Rudder profile terminology. Adapted from Cleynen (2011)

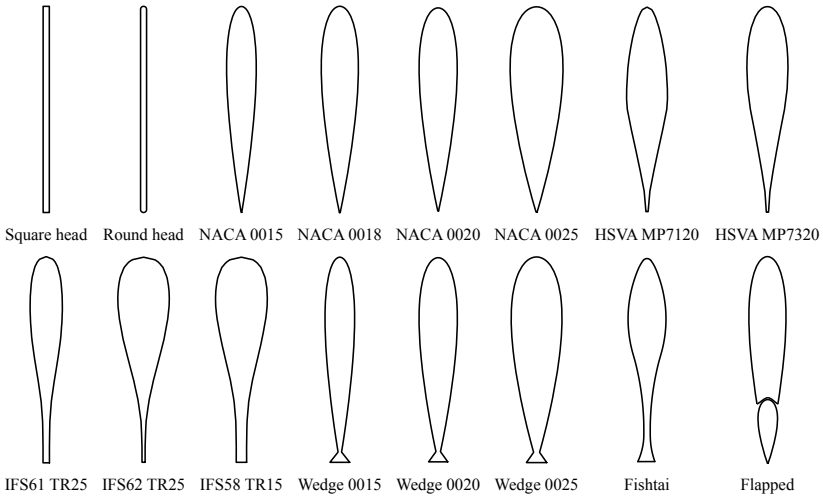

Figure 4: Typical rudder profiles, including flat-plate, NACA, HSVA, IFS, wedge-tail, fishtail, and flapped

head in Figure 4). Thieme (1965) indicated that the flat-plate profiles may achieve high efficiency in straight-ahead condition. Liu and Hekkenberg (2015) showed that this high efficiency only appears at small angles of attack, i.e. up to approximately 5°. After this, the lift coefficient stalls and the lift-to-drag ratio collapses. Additionally, flat-plate rudders stall at a smaller angle than other profiles due to earlier and stronger flow separation (Liu and Hekkenberg, 2015). At present, flat-plate rudders are frequently seen on small boats and antique inland vessels but not common for modern seagoing ships.

3.2. NACA

NACA profiles are the most widely applied rudder profiles (Kim et al., 2012) (Figure 4). They are also applied to other foil shaped structures such as, propellers Takekoshi et al. (2005), propeller ducts (Koç et al., 2011; Yılmaz et al., 2013), marine current turbines (Molland et al., 2004; Batten et al., 2006, 2008; Goundar et al., 2012), fins (Surendran and Kiran, 2006, 2007; Ram et al., 2015), and wind turbines (Bertagnolio et al., 2001; Timmer, 2010). Furthermore, the NACA series is the most thoroughly investigated aerofoil. Therefore, it is commonly taken as a benchmark case for both aerodynamic and hydrodynamic studies. The geometry of the NACA series was described by Ladson et al. (1996). Wind tunnel test results for aerofoils at small Mach numbers, which means the air is almost incompressible like water, are applicable for ship rudders (Loftin and Smith, 1949; Abbott and Von Doenhoff, 1959; Gregory and O'Reilly, 1970; Mccroskey, 1987; Ladson, 1988). Especially, characteristics of aerofoils with low aspect ratios (Fink and Lastinger, 1961; Pelletier and Mueller, 2000; Sathaye, 2004; Torres and Mueller, 2004) are quite close to those of common ship rudders. For ship rudders, Whicker and Fehlner (1958); Thieme (1965) carried out tests of the NACA profiles. In general, NACA profiles can generate sufficient manoeuvring force with a high efficiency (Liu and Hekkenberg, 2015). Liu et al. (2015, 2016) presented the manoeuvring performance of a KVLCC2 tanker with NACA rudders of various thickness.

3.3. HSVA

HSVA profiles were developed for ship rudders by Hamburg Ship Model Basin (Hamburgische Schiffbau Versuchsanstalt GmbH (HSVA), Hamburg, Germany), as shown in Figure 4. Considering the rudder working conditions, the HSVA series is designed to have a good pressure distribution reducing the onset cavitation (Kracht, 1989). Bertram (2012, p. 271) provided offsets of two main HSVA profiles, i.e. HSVA MP71-20 and HSVA MP73-20. Thieme (1965) and Brix (1993) presented hydrodynamic characteristics of the HSVA profiles in detail. According to Hollenbach and Friesch (2007), high-lift HSVA profiles may reduce the rudder area and achieve 1% fuel saving.

3.4. IFS

IFS profiles were developed to achieve a steep lift curve slope, a large stall angle, and a high maximum lift coefficient by Institute für Schiffbau, Hamburg, Germany, as shown in Figure 4. Bertram (2012, p. 271) showed the

offsets of three main IFS profiles, i.e. IFS58-TR 15, IFS61-TR 25 and IFS62-TR 25. Thieme (1965) presented wind tunnel tests of the IFS profiles. Compared to the HSVA profiles, IFS profiles may generate slightly more lift, induce more drag, and suffer less cavitation (Bertram, 2012, p. 297).

3.5. Fishtail

Fishtail profiles (Figure 4), also know as Schilling rudders (Schilling, 1963; Schilling and Rathert, 1978), are normally developed based on conventional NACA, HSVA, and IFS profiles with trailing tails. The concave part, where the original profile connects with the tail, is smoothed to have a better pressure distribution that delays stalling. Fishtail rudders can effectively generate lift improving the ship manoeuvrability. Therefore, they are frequently used on inland vessels. Van Nguyen and Ikeda (2013, 2014a) developed high-lift fishtail profiles by optimising the maximum rudder thickness and the trailing edge thickness. Hasegawa et al. (2006c) and Nagarajan et al. (2008) discussed the superiority of the fishtail rudder to the conventional Mariner rudder of course-keeping ability in windy conditions. However, very few studies have examined the fishtail profiles by experimental tests. In addition, offsets of the fishtail profiles are commonly not publicly available.

3.6. Wedge tail

Wedge-tail profiles are simplified fishtail profiles (Figure 4), which normally have a sharp concave point. Van Nguyen and Ikeda (2014b) indicated that wedge-tail rudder hydrodynamic characteristics are related to the size of the tail and the rudder thickness. Additionally, a wedge-tail rudder may be more efficient than a fishtail rudder with the same maximum thickness and trailing edge (Van Nguyen and Ikeda, 2014b). Through CFD simulations, Liu and Hekkenberg (2015) presented that the tested wedge-tail profiles can generate more lift than the tested flat-plate and NACA profiles with additional drag.

3.7. Flapped

Flapped profiles have a moveable flap which changes the profile camber (Figure 4). Therefore, flapped profiles can improve ship manoeuvring performance without affecting its cruising characteristics. The disadvantages of flapped rudders are large hinge moments, high mechanical complexity, and potential maintenance difficulties (Oppenheim, 1974). Two main properties of a flapped rudder are the flap-linkage ratio (the flap angle relative to the rudder chord line divided by the applied rudder angle) and the flap-area ratio (the sectional area of the flap divided by the total sectional area). Olson (1955) indicated that an increase in either the flap-linkage ratio or the flap-area ratio increases the lift coefficient, reduces the rudder efficiency, and shifts the centre of pressure to the rear in ahead condition while for the astern condition, the lift coefficient is decreased.

Bertram (2012, p. 284) described that flapped rudders may provide a much higher lift curve slope and 60 % to 70 % higher maximum lift compared to a conventional rudder of the same shape, size, and area. Olson (1955) reported a

30% flap NACA 0018 profile using a 1.5 flap-linkage ratio can generate 50% higher lift than an all-moveable rudder of equal area. Kerwin et al. (1972a,b), Kerwin et al. (1974), and Oppenheim (1974) indicated that a 20% flap NACA 66 profile may achieve 59% higher lift than the original NACA 66 profile. Kerwin et al. (1972a) showed that the drag coefficient at zero lift increases with the flap size. Kerwin et al. (1972a) concluded that even a small flap can largely increase the maximum lift coefficient. Additionally, the size of the flap in a range of 20 % to 50 % of the total rudder area does not much influence the maximum lift coefficient (Kerwin et al., 1972a).

However, the increase in maximum lift is achieved at the expense of a large increase in the drag and the hinge moment (Kerwin et al., 1972a,b). The flap balance may reduce the flap moment but it also significantly reduces the rudder induced side force (Kerwin et al., 1974). Thus, Kerwin et al. (1974) suggested that a rudder with small, unbalanced flap might achieve a balance of the improvement over the all-moveable rudder and the practical structural requirement. Champlain (1971) analysed the effects of the flap gap (the distance between the trailing edge of the skeg and the leading edge of the flap with zero flap deflection) on rudder hydrodynamic characteristics indicating that a larger open gap may achieve a better overall performance.

3.8. Recommendations for industry practices in the selection of the rudder profile

Through the previous reviews, it is clear that different rudder profiles have different hydrodynamic characteristics in the lift and drag coefficients, the slope of the lift curve, the stall angle, and the lift to drag ratio. Thieme (1965) and Molland and Turnock (2007) further compared the performance of various rudder profiles. Liu et al. (2015, 2016) proposed regression formulas to estimate the rudder normal force of different rudder profiles and analysed their impacts on ship manoeuvrability. These differences in the characteristics of the profile should be carefully considered in the rudder design. Furthermore, it is recommended to make a uniform definition of the shapes of wedge-tail and fishtail profiles to make research outcomes easier to verify and to expand upon the existing research. In general, the choice of the rudder profile depends on ship particulars, operational requirements of manoeuvring performance, and fuel conservation.

For seagoing ships which sail long distance and commonly have tug assistance for hard manoeuvring in the port area, the efficiency of the rudder may have a higher priority than the effectiveness. Thus, on the prerequisite of sufficient rudder force for course keeping and manoeuvring, highly efficient profiles are suggested, such as NACA, HSVA, and IFS. For ships mainly sail in constrained waterways like inland vessels, the effectiveness of the rudder is more crucial than efficiency. Therefore, high-lift profiles, including fishtail, wedge-tail, and flapped, are proposed. When the applicable rudder area is limited due to ship draught or water depth, high-lift profiles are also favourable. In the case of working boats like tugs, where the manoeuvrability of the ship is the key, the effectiveness can be the primary concern while the efficiency can be sacrificed. All things considered, lift is nearly always gained at the expense of drag. A wise decision of the rudder profile should coincide with the objective of the design of the ship.

4. Rudder properties

After a decision of the profile, detail rudder design of properties should be considered. Avoiding ambiguity, the rudder properties discussed in this paper are illustrated in Figure 5. These properties affect the rudder hydrodynamic characteristics and determine the effectiveness and the efficiency of the rudder. Main properties discussed in the following sections are area, thickness, span, chord, and aspect ratios. Sweep angles, taper ratios, and tip shape have relatively small influences on the rudder hydrodynamic characteristics (Molland and Turnock, 2007), therefore, they are briefly introduced here.

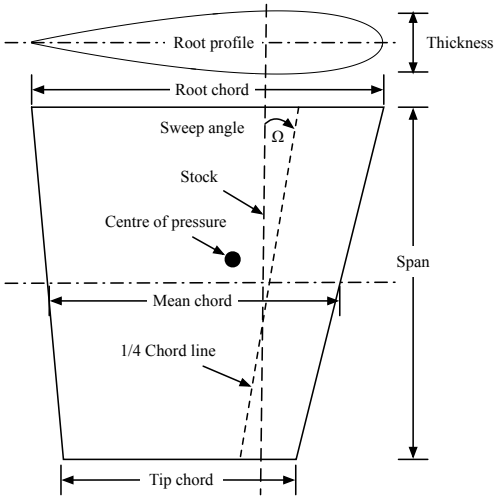

Figure 5: Rudder property terminology. Adapted from Molland and Turnock (2007, p. 72)

The sweep angle slightly affects the maximum lift coefficient and the stall angle (Molland and Turnock, 2002, p. 79). An increase in the taper ratio leads to an increase in the lift curve slope, the maximum lift coefficient, and the stall angle (Molland and Turnock, 2007, p. 90). A faired tip shape may reduce the minimum drag at a zero angle of attack, but it decreases the stall angle by 2° to 3° (Whicker and Fehlner, 1958). Hoerner (1965) and Molland and Turnock (2007) concluded that the square tip is better than the faired tip. Because the small advantage of the faired tip in the reduction of drag at small rudder angles is gained at the expense of large hydrodynamic losses at large rudder angles.

4.1. Area

The rudder area affects the amount of lift and drag induced by the rudder (Eq. 1). To generate the required manoeuvring forces and moments, the rudder (one or more) should have sufficient total area. Multiple rudders are applied when the area of a single rudder is not sufficient to turn the ship at the required rate. One reason why the rudder cannot have the required area is because the draught of the ship is small, e.g. in the case of inland vessels. However, a larger rudder area normally means larger rudder induced resistance.

The rudder area (A_R) or the total rudder area, if more than one rudder is applied, is commonly expressed as a ratio of the ship underwater lateral area ($L_{pp}T$), where L_{pp} is the ship length between perpendiculars and T is the fully loaded ship draught. The value of $A_R/L_{pp}T$ is normally first estimated based on similar ships or empirical formulas, and then optimised through iterations (Kim et al., 2012). Table 1 summaries the reference $A_R/L_{pp}T$ values found in literature (China Classification Society, 2003; Barrass, 2004; Molland and Turnock, 2007; Kim et al., 2012). The reference values in Table 1 indicate that ships which have high requirements of manoeuvrability, such as warships, pilot vessels, tugs, and trawlers, need large rudder area.

Table 1: Reference ratios of the rudder area to the ship lateral area ($A_R/L_{pp}T$) for different ship types

Ship types	$A_R/L_{pp}T$ [%]
Container ships	1.2 to 1.7 (Barrass, 2004, p. 88)
Passenger liners	1.2 to 1.7 (Barrass, 2004; Kim et al., 2012, p. 88)
General cargo ships	1.5 (Barrass, 2004, p. 88)
Single-propeller merchant ships	1.6 to 1.8 (Molland and Turnock, 2007, p. 189)
Twin-propeller merchant ships	1.6 to 2.2 (Molland and Turnock, 2007, p. 189)
Small cargo ship	1.7 to 2.3 (Kim et al., 2012)
Large cargo ship	2.0 to 2.8 (Kim et al., 2012)
Oil tankers and bulk carriers	2.0 (Barrass, 2004, p. 88)
Lake steamers	2.0 (Barrass, 2004, p. 88)
Cross channel ferries (RoRo ships)	2.0 to 3.0 (Barrass, 2004, p. 88)
Coastal vessels	2.0 to 3.3 (Barrass, 2004, p. 88)
Warships	2.4 to 2.8 (Molland and Turnock, 2007, p. 189)
Pilot vessels	2.5 to 4.0 (Barrass, 2004, p. 88)
Tugs	3.0 to 4.0 (Molland and Turnock, 2007, p. 189)
Trawlers	3.0 to 4.0 (Molland and Turnock, 2007, p. 189)
Inland cargo vessels in non-rapid stream segment	2.0 to 3.0 (China Classification Society, 2003, p. 11)
Inland cargo vessels in rapid stream segment	4.5 to 5.0 (China Classification Society, 2003, p. 11)

For rudders working directly behind propellers, Det Norske Veritas (2000) suggested that $A_R/L_{pp}T$ should not be less than:

$$\frac{A_R}{L_{pp}T} = 0.01\left[1 + 50C_B^2\left(\frac{B}{L_{pp}}\right)^2\right], \tag{3}$$

where C_B is the ship block coefficient and B is the ship beam. Additional 30% area should be added if the rudder does not work directly behind a propeller (Det Norske Veritas, 2000). According to Shiba (1960), Molland and Turnock (2007, p. 191) concluded that the rudder effectiveness (a decrease in ship turning diameter and transfer) improves with an increase in the rudder area up to about $A_R/L_{pp}T = 0.025$.

To ensure a quick response to helm for broad ships, Schneekluth and Bertram (1998, p. 62) advised relating the rudder area to the ship midship section area (A_m) and the rudder area should not be less than 12% of A_m. To satisfy a particular turning index, Clarke et al. (1983) reported that as C_B increases the rudder area increases slightly while as the ratio of the ship beam (B) to the ship length (L_{pp}) increases the rudder area increases significantly, especially above B/T larger than 3.0. Thus, inland vessels which typically have larger block coefficients, much larger L_{pp}/B ratios, and extremely much larger B/T ratios than seagoing ships (Quadvlieg, 2013) should carefully consider the size of each rudder and the number of rudders to have sufficient total rudder area.

4.2. Thickness

The rudder thickness (T_R), which is commonly expressed as a ratio of the rudder chord length as T_R/C_R, needs to satisfy the structural needs considering the hydrodynamic characteristics. It affects the minimum drag, the stall angle, and the maximum lift coefficient (Molland and Turnock, 2007, p. 92). Commonly, thinner profiles have higher efficiency, i.e. a higher lift to drag ratio, than thicker profiles. Van Beek (2004) indicated that a slim rudder profile may increase the propulsive efficiency by 1 % to 3 %. Liu et al. (2015, 2016) carried out CFD simulations of five NACA profiles presenting that thinner NACA profiles are more effective and efficient than thicker NACA profiles. Sometimes, a rudder may have span-wise different thickness, for instance, a thin profile at the tip and linearly increases to a thick rudder profile at the root or vice verse. This configuration may provide a balance of the structural requirement and the hydrodynamic efficiency.

4.3. Span and chord

The rudder span or rudder height (B_R) is the distance between the rudder root and tip sections. Normally, the span is expected to be as large as possible, which may ensure a large geometric rudder aspect ratio for high effectiveness and efficiency. However, the span is commonly constrained by ship particulars (ship draught) and operational profiles (water depth). From observation and experience, a normal value of the rudder span is around the size of the propeller diameter. The rudder chord or length (C_R) is the distance between the leading and trailing edges. The chord is commonly determined according to the rudder area, the geometric aspect ratio, and the span. For unbalanced rudders, a large chord is not favourable as it may put an excessive burden on the steering gear.

4.4. Geometric and effective aspect ratios

Rudder aspect ratios have the most significant influence on rudder hydrodynamic characteristics (Molland and Turnock, 2007, p. 89). It concerns two concepts: the geometrical aspect ratio (Λ_G) and the effective aspect ratio (Λ_E). Λ_G is commonly expressed as $\Lambda_G = B_R/C_R$ or $\Lambda_G = B_R^2/A_R$. The effective aspect ratio (Λ_E) is the actual aspect ratio applied for hydrodynamic force calculation. In general, a rudder with a larger geometric aspect ratio can generate larger lift and lower drag (Whicker and Fehlner, 1958). However, a small geometric aspect ratio may enhance the manoeuvrability with a large stall angle (Molland and Turnock, 2007, p. 64). Confirmed by rudder manufactures, a common range of geometric aspect ratios for seagoing ships is 1.5 to 3 while the common range of aspect ratios for inland vessels is 1 to 2.

To compare the profile hydrodynamic characteristics, an infinite geometric aspect ratio, i.e. an infinite span, is commonly assumed in experimental and numerical studies (Harris, 1981; Mccroskey, 1987). Such an approach associates the hydrodynamics only with the properties of the 2D profile rather than the 3D shape of the rudder. Thus, it is useful for investigating the profile drag, the pressure distribution, and the theoretical application (Molland and Turnock, 2007, p. 41). In practice, the rudder has a finite span and a finite aspect ratio. A finite span has a downward flow along and behind the rudder, which is the so-called downwash. This downwash is combined with the inflow leading to a smaller effective angle of attack than the deflected rudder angle. Therefore, a small geometric aspect ratio has a larger reduction of the effective rudder angle due to a larger downwash leading to a larger stall angle.

The effective aspect ratio (Λ_E) is commonly estimated based on the geometric aspect ratio (Λ_G) as $\Lambda_E = k_\Lambda \Lambda_G$, where k_Λ is the ratio of Λ_E to Λ_G. When the rudder root is sufficiently close to a flat surface, such as a large end plate or a flat hull, k_Λ is close to 2 owing to the ideal image mirror effect (Molland and Turnock, 2007, p. 183). Considering the gap effects, Brix (1993, p. 97) provided reference values of k_Λ. Root and tip end plates may increase the effective aspect ratio but also causes notable drag. From observation, seagoing ship rudders normally do not have end plates while inland vessel rudders tend to have both root and tip plates to enlarge the effective aspect ratio.

4.5. Recommendations for practical selection of the rudder properties

Besides the rudder profile, the rudder properties specify how the rudder is shaped in three dimensions. The rudder performance is the end product of all these properties. First of all, the total area should be sufficiently large as it is a determinant factor of the amount of rudder force. The reference values of the total area are given in Table 1. When the area of a single rudder is not sufficient, multiple-rudder configurations are recommended for inland vessels because of the limited ship draught and seagoing ships due to the enlargement of the ship dimensions. In addition, the increase in the total rudder area leads to an improvement in the ship manoeuvrability but makes the rudder induced resistance larger. Therefore, for ships with large rudder area, the selection of the rudder profile becomes even more crucial as discussed in the last section.

As a general rule, thinner rudders have better hydrodynamic performance than thicker ones. The structural requirement and the hydrodynamic performance have to be considered in coincidence in the determination of the rudder thickness. With a prerequisite of the total rudder area, large span means short chord, furthermore, a large geometric aspect ratio, which is desirable for both efficiency and effectiveness. The span, the chord, and the geometric aspect ratio are commonly limited in a routine range, but the effective aspect ratio can be enlarged by adding end plates on the tip and the root of the rudder. Yet, very few studies have examined the impacts of the shape and the size of the end plates on the rudder hydrodynamics. As a summary, emphasising the ship manoeuvrability, large total rudder area, small thickness, large span, short chord, large geometric and effective aspect ratios are recommended.

5. Rudder types

Conventionally, ships sail with a propeller and a rudder aft of the propeller, which is the so-called propeller-rudder system (PRS). The PRS is regarded as a passive steering device and widely applied for nearly all ship types. A PRS may have either a ducted propeller or an unducted propeller. The rudder in a PRS is classified based on two aspects: the position of the stock (unbalanced, semi-balanced, or balanced) and the structural rudder-hull connection (the number of pintles, without skeg, semi-skeg, or full-skeg). The choice of the rudder type depends on the ship type, the ship main dimensions, the shape of the stern, and the require rudder size (Molland and Turnock, 2007, p. 13). This section reviews four common rudder types, i.e. unbalanced, fully-balanced, spade, and semi-skeg, which are shown in Figure 6.

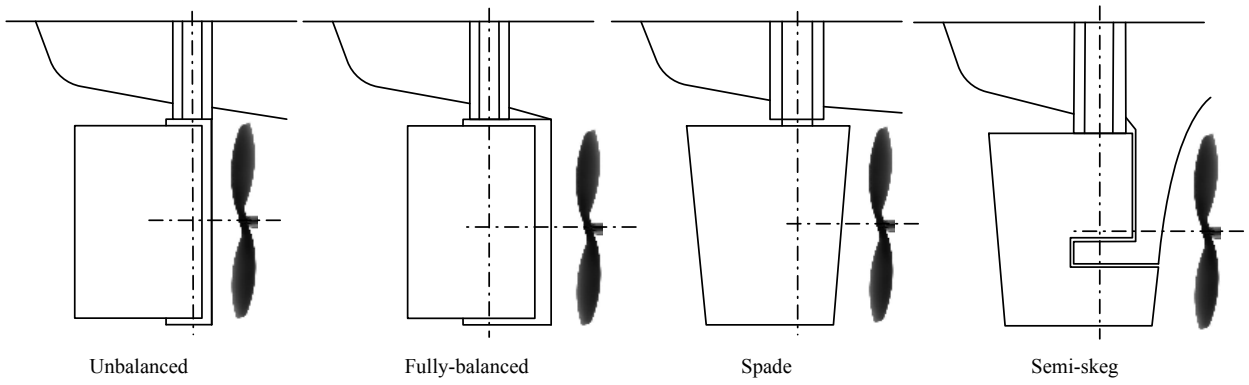

Figure 6: Common rudder types in conventional propeller-rudder systems. Adapted from Molland and Turnock (2007, p. 15)

5.1. Unbalanced rudders

The unbalanced rudder has its stock at the leading edge making the entire area after the stock (Figure 6). The steering gear has to provide all the rudder turning torque. It implies that this solution only works for the rudder with a limited area, because otherwise the rudder cannot be steered properly. To compensate the large bending moment, an

unbalanced rudder has two pintles on the tip and the root. This arrangement protects the rudder from damage even in the case of grounding. Currently, unbalanced rudders are not widely used for modern ships. But they are still popular for small crafts and fishing vessels as the unbalanced rudders are easy and cheap to produce (Bertram, 2012, p. 282).

5.2. Fully-balanced rudders

The fully-balanced rudders or more commonly named as the balanced rudder has its rudder stocks at 20 % to 40 % chord length from the leading edge (Figure 6). The water force acting on the aft part of the rudder is partially or, at some rudder angles, completely compensated by the force acting on the forward part of the rudder. Therefore, the rudder turning torque and required capacity of the steering gear for the fully-balanced rudder are far less than that for the unbalanced rudder. Since the action point of the force changes with the applied rudder angle, it is not feasible to maintain the balance over a complete range of rudder angles. Fully-balanced rudders have been extensively applied to single-propeller merchant ships and gradually superseded by semi-balanced skeg rudders (Molland and Turnock, 2007, p. 14).

5.3. Spade rudders

The spade rudder is a kind of balanced rudders with a taper ratio (Figure 6), i.e. the ratio of the root chord to the tip chord. Rudders with large taper ratios may reduce the rudder drag or even generate thrust (Carlton et al., 2009). Due to the large bending moment, the spade rudder commonly requires a large stock diameter and large rudder thickness. According to Bertram (2012, p. 283), spade rudders are not feasible if the required stock diameter is larger than 1 m. Like balanced rudders, spade rudders require less energy than unbalanced rudders. Therefore, the investment cost of motors and actuators are reduced. Meanwhile, the fuel consumed by the steering gear is lower.

According to Bertram (2012, p. 272), spade rudders are more favourable than unbalanced or fully balanced rudders. From the hydrodynamic and cavitation points of view, spade rudders are better than semi-skeg rudders. At an optimum relative position to the propeller (about 30 % to 35 % of the propeller diameter), a spade rudder shows about 1.6% gain of power against the semi-skeg rudder (Minchev et al., 2013). Unlike semi-skeg or full-skeg rudders, spade rudders do not have gap cavitation, thereby reducing the time and cost for maintenance. Nowadays, spade rudders are widely applied for all ship types.

5.4. Semi-skeg rudders

The semi-skeg rudder, also called the horn rudder, or the Mariner rudder, is a kind of semi-balanced rudder, i.e. unbalanced root part with skeg and balanced tip part without skeg (Figure 6). The location of the pintle is supposed to be in the vicinity of the centre of pressure affecting the response and torque characteristics of the rudder. The horn provides structural support for the span-wise bearing moment making a large rudder area possible. In addition, the

semi-skeg rudder requires less turning torque than the unbalanced rudder and has less bending moment than the spade rudder. Nowadays, the semi-skeg rudder tends to be favourable for new built large ships, for instance, Very Large Container Ships (VLCS), despite the hydrodynamic advantages of the spade rudder (Lübke, 2009).

Through series of free-stream wind-tunnel tests, Molland (1977, 1978) found that a semi-skeg rudder has a little smaller maximum lift, a smaller lift to drag ratio, and a significantly smaller lift curve slope than an all-moveable rudder of the same size. Thus, the semi-skeg rudder is less effective than the spade rudder for manoeuvring (Bertram, 2012, p. 283). These changes in lift and drag coefficients are mainly caused by the rudder horn. Even though the rudder horn itself does not incline, it still significantly affects the lift and the total drag of the rudder (Lübke, 2009).

5.5. Recommendations of the decision in the rudder type

As a summary, conventional propeller-rudder systems still hold a dominant position on merchant ships. Even though active steering devices have been developing rapidly for offshore engineering, the conventional rudders can still provide extraordinary performance regarding bollard pull, response times, and cruise behaviour (Lehmann, 2012). Following consideration of the rudder type, spade rudders and semi-skeg rudders are primarily contemporary design choices. From the perspective of hydrodynamics, spade rudders are better than semi-skeg rudders for ship manoeuvrability and fuel consumption. Thus, it is proposed to take the spade rudder as a first choice. However, the area of a spade rudder is limited due to high bending moment. Therefore, semi-skeg rudders are recommended for large ships which require a large rudder area.

6. Interactions among the hull, the propeller, and the rudder

The propeller accelerates and rotates the wake of the hull to the rudder. The rudder works in the propeller slipstream, inducing manoeuvring forces and moments. The upstream propeller affects the rudder induced manoeuvring force while the presence of the rudder influences the propeller generated thrust and the required torque (Turnock, 1993). These interactions affect the total effectiveness and efficiency of the ship (Minchev et al., 2013). This section discusses the interactions among the hull, the propeller, and the rudder in four aspects: the flow straightening effect, the propeller slipstream, the relative position of the propeller and the rudder, and the multiple rudders.

6.1. Flow straightening effect

When the ship is drifting at certain drift angle (β), the effective rudder angle (α_R) decreases. However, the hull straightens the inflow into the propeller-rudder system recovering the loss of the effective rudder angle. Figure 7 illustrates the terminology applied in the flow straightening effect.

The relationship of the terminology is as follows:

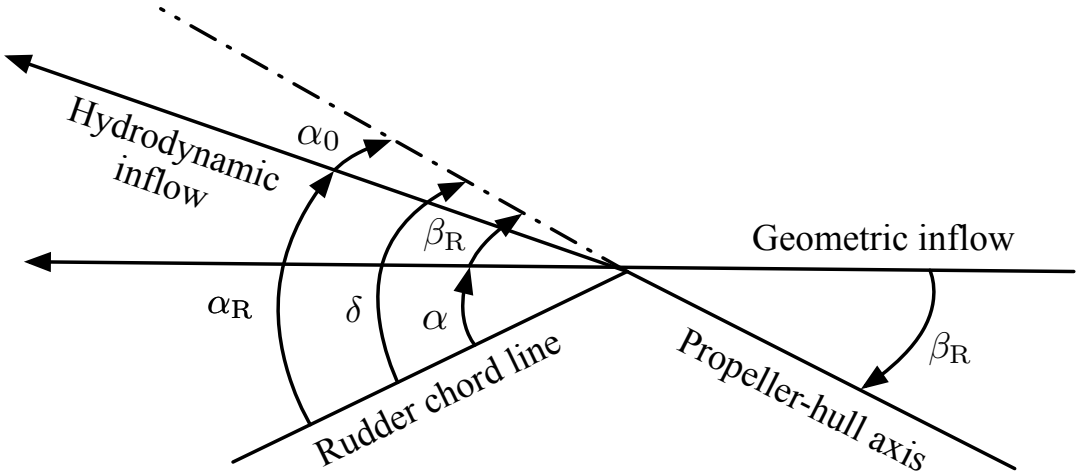

Figure 7: Flow straightening terminology. Adapted from Molland and Turnock (1995a); Badoe et al. (2015)

$$\delta = \alpha + \beta_R = \alpha_R + \alpha_0 = \alpha_R + \gamma_R \beta_R, \tag{4}$$

where δ is the rudder angle relative to the ship centreline, α is the geometric rudder angle, α_0 is the incidence for zero lift, β_R is the drift angle at the position of the rudder which is larger than the ship drift angle β, and γ_R is the flow straightening factor. γ_R depends on the form of the hull body, the drift angle, and the propeller working load (Molland and Turnock, 2002). The magnitude of the drift angle effect on the rudder performance depends on the advance ratio or propeller working load. A lower advance ratio leads to a higher propeller working load and more significant flow straightening influence. The drift angle shifts but does not greatly change the shape of the rudder force coefficient curve (Molland and Turnock, 1995b).

6.2. Propeller slipstream

The propeller advance ratio (J_P), which expresses the speed of the propeller slipstream compared to the ship velocity, is calculated as follows:

$$J_P = \frac{V_P}{n_P D_P}, \tag{5}$$

where V_P is the propeller advance speed, n_P is the propeller resolution, D_P is the propeller diameter. A high J_P (low or zero propeller thrust) indicates that the rudder performance depends on the hull, the free surface, and the ship yaw angle while a low J (high propeller thrust) indicates the rudder induced forces is determined by the propeller slipstream (Turnock, 1993). The propeller working load K_T/J_P^2 forms the speed and the pressure distribution of the propeller slipstream. An increase in the propeller working load increases the rudder induced side force while delays

the stall angle (Molland and Turnock, 1991, 1993a; Turnock, 1993). Meanwhile, the presence of a rudder behind the propeller increases the propeller working load (Simonsen, 2000, p. 155).

Rudder hydrodynamic characteristics tested in open water are different from those tested in the propeller slipstream. Oppenheim (1974) found that the lift curve slope, the maximum lift coefficient, the stall angle, and the drag coefficient increase when the rudder is tested in the propeller slipstream. For spade rudders, Nienhuis (1987) showed that the stall angle is significantly delayed in the propeller slipstream but the slope of the lift curve is not much affected. Kerwin et al. (1974) compared the rudder hydrodynamics of a 20% flap rudder in propeller slipstream and uniform flow indicating that the rudder lift curve slope is increased by about 25%.

6.3. Relative positions of the propeller and the rudder

The relative positions of the propeller and the rudder are described by longitudinal (x_{PR}), lateral (y_{PR}), and vertical (z_{PR}) separations. The relative positions determine the proportion of the rudder area in the propeller slipstream, which in fact influences the rudder induced side force (Molland and Turnock, 1991). Stierman (1989a,b) indicated the dominant impact factors considering the propeller-rudder interaction are the propeller pitch ratio, the rudder thickness, and the longitudinal propeller-rudder separation.

The longitudinal separation (x_{PR}) is the distance between the rudder stock and the propeller rotating plane. It determines the diameter and the velocity distribution within it of the propeller slipstream arriving at the rudder (Turnock, 1993). According to Molland and Turnock (1991), x_{PR} has little impacts on the rudder side force. Oppenheim (1974) concluded that the steady forces on the rudder are completely independent of x_{PR} in the range of $0.5\,D_P$ to $1.0\,D_P$. x_{PR} also affects the rudder induced resistance. Under some extraordinary conditions, the rudder may generate thrust reducing the overall resistance of the ship (Carlton et al., 2009). At various ship speeds, Reichel (2009) tested six rudders at x_{PR} of $0.59\,D_P$, $0.65\,D_P$ and $0.71\,D_P$ and concluded that the best rudder location is the closest to the propeller. Minchev et al. (2013) tested spade and semi-skeg rudders at x_{PR} of $0.456\,D_P$, $0.371\,D_P$ and $0.272\,D_P$ and showed that the optimum x_{PR} for a single-propeller single-rudder bulk carrier could be in the range of $0.30\,D_P$ to $0.35\,D_P$.

The lateral separation (y_{PR}) is the distance between the rudder stock and the propeller shaft. When the number of propellers and the number of rudders are the same, the rudder central plane commonly aligns with the propeller shaft. A change in y_{PR} leads to a shift in the rudder incidence for zero lift while the hydrodynamic characteristics are not greatly affected (Molland and Turnock, 1992, 1993b; Turnock, 1993; Molland et al., 1995; Jurgens, 2005). In addition, this shift increases with an increase in the propeller working load (Molland et al., 1995). The vertical separation (z_{PR}) is the distance between the rudder tip and the propeller shaft. A change of z_{PR} alters the proportion of the rudder span in the propeller slipstream leading to a shift in the incidence of zero lift. In general, the vertical separation has relative small influences on the rudder performance.

Both experimental and numerical methods have been applied for the studies on the propeller and the rudder.

Turnock (1990) described a wind-tunnel test rig for the propeller-rudder interaction effect. This test rig has been successively applied for experimental tests (Molland and Turnock, 1991, 1992, 1993a,b, 1995b; Molland et al., 1995; Molland and Turnock, 2002). Shen et al. (1997b), Felli et al. (2009), Felli and Falchi (2011), and Pecoraro et al. (2015) carried out Laser Doppler Velocimetry (LDV) measurements. Turnock and Wright (2000), Laurens (2003), Lee and Fujino (2003), Natarajan (2003), Phillips et al. (2010), Caldas et al. (2011), Di Mascio et al. (2015), and Badoe et al. (2015) presented CFD studies on the propeller-rudder interactions. Stuck et al. (2004) performed an evaluation of the RANS method for predication of steady rudder performance. In addition, the rapid development of CFD provides new possibles of full-scale tests avoiding the challenge of scaling *Re* as mentioned in Section 2.

6.4. Multiple rudders

When multiple rudders are applied, the interaction among the rudders should be considered. Multiple-rudder ships may have different starboard-side and port-side manoeuvring behaviours. The asymmetrical behaviours are notable for single-propeller twin-rudder ships (Hamamoto and Enomoto, 1997; Hasegawa et al., 2006b; Nagarajan et al., 2009; Di Mascio et al., 2011; Kang et al., 2011; Broglia et al., 2013). According to Yoshimura and Sakurai (1989), hydrodynamic characteristics of a twin-propeller twin-rudder are not so much different from those of a single-propeller single-rudder ship. Quite a few studies have been done for twin-propeller twin-rudder ships (Yoshimura and Sakurai, 1989; Lee et al., 2003; Yoo et al., 2006; Kim et al., 2007; Kang and Hasegawa, 2007; Khanfir et al., 2008, 2009; Tabaczek, 2010; Khanfir et al., 2011; Dubbioso and Viviani, 2012; Coraddu et al., 2013; Bonci et al., 2015; Dubbioso et al., 2015). Additionally, the hydrodynamic characteristics of each rudder in twin-rudder configurations is also affected by the interaction between the rudders (Gim, 2013; Liu and Hekkenberg, 2015).

For twin-rudder ships, the distance between the rudder stocks and the coupling of the rudder angles may have significant impacts on ship manoeuvrability. By setting both rudders outwards at 75°, covering the gap between the leading edges, a twin-rudder ship may reduce the stopping distance by 50% compared to a conventional reverse engine stopping (Baudu, 2014, p. 41). These outward rudder angles are called clam shell angles as shown by Hamamoto and Enomoto (1997) and discussed by Hasegawa et al. (2006a). Hamamoto and Enomoto (1997) proposed analytical formulas of the ship forward speed drop, the stopping time, and the stopping distance when a ship stops with the clam shell angles. Although the above studies invested the manoeuvrability of some twin-rudder seagoing ships, no reference in the literature described the manoeuvring performance of multiple-rudder inland vessels. In fact, inland vessels are more commonly equip twin rudders or even quadruple rudders than seagoing ships.

6.5. Recommendations for further research on the hull-propeller-rudder interactions

As a rule, the interactions among the hull, the propeller, and the rudder affect the rudder hydrodynamic characteristics. The flow straightening effect influences the effective rudder angle, which is important for the calculation of

the rudder induced force in manoeuvring simulations. However, in the existing literature, the flow straightening factor is primarily determined by model tests. More research is needed to better understand the roles of the impact factors on the flow straightening effect. Furthermore, it is proposed to generate regression formulas of the flow straightening factor through series of benchmark tests.

The propeller slipstream mainly delays the stall angle. It may maintain or change the slope of the lift curve depending on the working load of the propeller. Further research in this field would be of great help in manoeuvring simulations. The relative position of the propeller and the rudder influences the performance of both the propeller and the rudder. With extra consideration of cavitation, it is recommended to put the rudder as close as possible to the propeller. Moreover, interaction among multiple rudders requires further study, which is particularly meaningful for inland vessels.

Last but not least, both experimental and numerical methods are applicable for studies on the propeller and the rudder, which provide lots of possibilities for the further research. It is recommended to use numerical methods for primary studies and apply experimental tests as a final check. Additionally, benchmark experimental tests are needed for the validation of the numerical methods.

7. Rudder performance

Good performance in ship manoeuvrability, fuel consumption, and cavitation is the goal of the rudder design. Above all, rudders should be capable of inducing sufficient manoeuvring force to ensure the navigations safety, especially for ships which frequently sail in constrained waterways or severe conditions. The rudder should also be efficient, which means minimum drag at the required lift. Last but not least, the cavitation performance should be considered to reduce the time and cost of maintenance and repairs.

7.1. Ship manoeuvrability

The rudder effectiveness in ship manoeuvrability is commonly evaluated by the amount of the rudder induced side force (Y_R), which is the component of the rudder resultant force normal to the ship centreline (Brix, 1993, p. 96). Y_R can be calculated as follows:

$$Y_R = 0.5\rho V_R^2 A_R C_{YR}, \tag{6}$$

where C_{YR} is the rudder side force coefficient and is normally estimated based on the gradient of the side force coefficient C_{YR_α} as $C_{YR} = \alpha C_{YR_\alpha}$. Furthermore, C_{YR_α} becomes available from experimental results or empirical formulas as follows:

$$C_{YR_\alpha} = \frac{1.8\pi\Lambda_E}{\sqrt{\Lambda_E^2 + 4} + 1.8}, \text{ by Mandel (1967);} \tag{7}$$

$$C_{YR_\alpha} = \frac{2\pi\Lambda_E(\Lambda_E + 1)}{(\Lambda_E + 2)^2}, \text{ by Söding (1982).} \tag{8}$$

More frequently, the rudder side force is calculated by the rudder normal force (N_R), neglecting the rudder tangential force (T_R) (Kijima et al., 1990; Yasukawa and Yoshimura, 2014) as follows:

$$Y_R = -(1 + a_H)N_R \cos\delta, \tag{9}$$

where a_H is the rudder force increase factor due to the hull. The rudder normal force (N_R) is expressed as:

$$N_R = 0.5\rho V_R^2 A_R f_\alpha \sin\alpha, \tag{10}$$

where $f_\alpha \sin\alpha$ stands for the rudder normal force coefficient (C_N). According to Fujii (1960) and Fujii and Tsuda (1961, 1962), f_α is commonly estimated as follows:

$$f_\alpha = \frac{6.13\Lambda_G}{\Lambda_G + 2.25}. \tag{11}$$

However, Eq. 11 does not account the effects of the rudder profile and the number of rudders on the rudder hydrodynamic coefficients. Considering the characteristics of the rudder profile, Liu et al. (2015, 2016) proposed regression formulas for the normal force coefficients of various profiles based on CFD results. Furthermore, Liu and Hekkenberg (2015) showed that each rudder of a twin-rudder configuration has different hydrodynamic coefficients. Motoki et al. (2015) discussed the effects of the rudder horn and the propeller vortex on manoeuvring simulations. According to Bertram (2012, p. 272), the rudder effectiveness can be improved through the following methods:

- Increase the percentage of the rudder surface in the propeller slipstream.
- Increase the total rudder area.
- Apply more suitable rudder types (e.g. the spade rudder instead of the semi-skeg rudder).
- Apply more powerful rudder engines allowing larger rudder angles than the customary maximum rudder angle of 35°.
- Higher rudder turning speed.

7.2. *Fuel consumption*

A rudder may increase about 1% total resistance in the neutral position and 2 % to 6 % total resistance at moderate angles (Alte and Baur, 1986). Aiming to cut CO_2 emissions, the International Maritime Organization (IMO) requires that all ships larger than 400 gross tonnage reduce Energy Efficiency Design Index (EEDI) by up to 30% after 2025 (International Maritime Organization, 2011, 2012). To achieve such a goal, more efficient rudders, which can induce sufficient lift with minimum drag, are helpful. Furthermore, minimised rudder torque can also reduce the fuel consumed by the steering gear. In general, 2 % to 8 % saving can be achieved by optimising the rudder in profiles and types (Hochkirch and Bertram, 2010).

Hochkirch and Bertram (2010) pointed out that the rudder has an underestimated potential for fuel reduction, for instance, reducing the rudder size (weight and resistance) by improving the rudder profile or changing to an efficient flapped rudder. Lehmann (2007) summarised that an efficient rudder system should have a slim and low drag rudder profile, generate high lift at small rudder angles, have a smooth surface, be tuned with the propeller, be light weighted, and be easy to maintain. Hollenbach and Friesch (2007) listed the possible maximum gains of fuel reduction by optimising the arrangement and shape of the propeller-rudder system. For instance, highly efficient rudders may increase the propulsive efficiency by 6% (Hollenbach and Friesch, 2007).

Lehmann (2007) suggested optimising the propeller-rudder system and reducing the rudder weight to save fuel. Lehmann (2007) indicated that it is important to integrate rudders with propeller and hull form design. Van Beek (2004); Lehmann (2007) applied a torpedo shaped bulb on the rudder as a streamlined continuation of the propeller hub. Similarly, Hollenbach and Reinholz (2011) found that rudders with a rudder bulb require 4% less power than the standard rudder. Sarasquete et al. (2012) showed a 12% reduction of power demand for a fishing vessel by modifying the propeller hub and rudder shapes.

Reducing unnecessary drag due to rotating incidence flow, a twisted rudder may enhance the overall propulsive efficiency. Commonly for a clockwise rotating propeller, the leading edge above the shaft centre is twisted port and below the shaft is twisted starboard. A twisted rudder with a bulb may have 4% less fuel consumption (Hollenbach and Friesch, 2007). Kim et al. (2014) reported that a Z-twisted rudder, which has a Z-shape leading edge, with and without a fin may reduce the fuel consumption by 2.35% and 2.95%, respectively. Due to a decrease in the effective angle of attack, the lift and drag of the twisted rudder may be smaller than the common spade rudder (Kim et al., 2014). Yang et al. (2015) further studied the rudder force of a twisted rudder.

7.3. *Rudder cavitation*

Rudders are placed in high-speed propeller slipstream. Cavitation happens when the pressure in the flow is as low as the water vapour pressure. Brennen (1995, Section 3.6) explained that the cavitation damage is caused by the repetition of cavitation bubble collapse in the vicinity of a solid surface. This collapse generates highly localised and

transient surface stresses, which causes local surface fatigue failure and eventually develops to erosion. Due to repair or replacement of the eroded rudder, maintenance cost increases and operational time decreases (Shen et al., 1997a). Meanwhile, the cavitation also causes an increase in drag, hull vibration, and radiated noise (Shen et al., 1997a).

The enlargement of ships and the increase in ship speed lead to higher speed and lower pressure in the propeller slipstream. The rudder cavitation has become more and more serious (Han et al., 2001; Ahn et al., 2012). As the service speed tends to be decreased to save fuel and meet the EEDI requirements (Hollenbach and Friesch, 2007; Lehmann, 2007; Hochkirch and Bertram, 2010). The cavitation may become less significant in the future. As Rhee et al. (2010) showed, Figure 8 illustrates the typical areas of cavitation damage on a semi-skeg rudder. The damages are mainly due to the high speed near the horn and pintle section gaps, the propeller tip and hub vortex, and the propeller sheet.

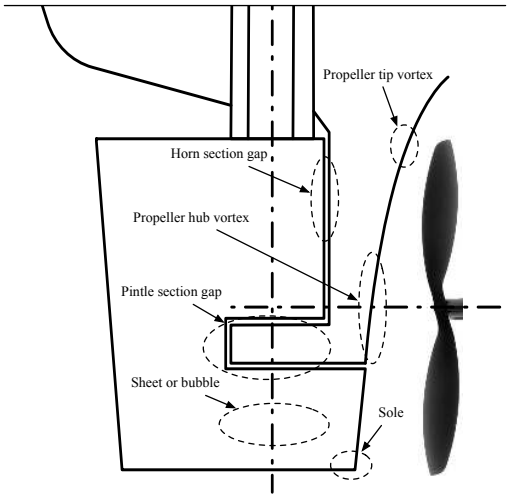

Figure 8: Typical areas of cavitation damage on a semi-skeg rudder. Adapted from (Rhee et al., 2010)

Cavitation causes cavity drag. The cavity drag increases sharply with an increase in ship speed (Shen et al., 1997a). Thus, a reduction of ship resistance is expected if the rudder can be operated without cavitation, especially for high-speed vessels. Lübke (2009) showed that cavitation effects cause a 10% decrease in lift and a 20% increase in drag. According to Shen et al. (1997b), Mewis and Klug (2004), and Ahn et al. (2012), twisted spade rudders can reduce the cavitation and improve the propulsion efficiency. Ahn et al. (2012) reported an X-Twisted rudder which can reduce the rudder cavitation and improve the overall manoeuvrability.

7.4. Recommendations for improvements of the rudder performance

As reviewed in the previous sections, the rudder performance can be roughly judged in three aspects: ship manoeuvrability that relates to navigation safety, fuel consumption that affects transport efficiency, and rudder cavitation

that determines operation and maintenance cost. The keys to improving the effectiveness of the rudder in ship manoeuvrability are increasing the rudder inflow velocity or the percentage of the rudder area in the propeller slipstream, enlarging the total rudder area, and improving the rudder hydrodynamic characteristics by changing the profile, the property, and the type. However, the improvement in the ship manoeuvrability commonly comes at the expense of extra rudder induced resistance. Future research should, therefore, concentrate on the investigation of energy saving methods of the rudders such as the twisted rudders and the energy saving bulbs. Considering the cavitation, whole-body profiles and types like the spade rudder with a NACA profile have advantages over the separated ones like the semi-skeg rudder with a flapped profile. Even though for common commercial ships, the effectiveness and efficiency of the rudder get higher priority than the cavitation in the design process, a final check of the rudder performance in the cavitation cannot be neglected.

8. Conclusions

Rudders are important for ship course keeping and manoeuvring. A good rudder should be effective in manoeuvring force generation ensuring ship navigation safety. Considering fuel consumption, the rudder should also be efficient, i.e. induce minimum resistance with sufficient manoeuvring force. Furthermore, the cavitation performance should be considered to reduce the potential maintenance cost and reduction in operational time. Besides the facts that active steering devices are increasingly applied in offshore engineering and special vessels, conventional propeller-rudder systems are still the main steering devices.

Rudder hydrodynamics (lift and drag coefficients) are closely related to the working conditions (Reynolds numbers and angles of attack). Thus, in the application of model-scale results, which are commonly obtained in different conditions from reality, to full-scale ships, extra corrections should be taken. Furthermore, practical operational profiles should be considered in rudder design. The rudder type affects the rudder performance and depends on the practical requirements of size and structure. Spade and semi-skeg rudders are the main contemporary choices. Spade rudders are better in the hydrodynamic and cavitation performance than semi-skeg rudders while semi-skeg rudders are superior in bending moment and turning torque to spade rudders.

Rudder profiles largely affect the rudder hydrodynamic characteristics. High-lift profiles, such as wedge-tail, fishtail, and flapped profiles, improve the rudder effectiveness while cause additional drag. However, very few studies have examined the high-lift profiles and their impacts on ship manoeuvrability. NACA, HSVA, and IFS profiles are highly efficient and thus suggested for large seagoing ships. Furthermore, principle rudder properties are the rudder area and the rudder aspect ratios, which determine the magnitude of the rudder force. Sufficient rudder area should be ensured. When the area of a rudder is limited, multiple rudders are suggested. Yet, few studies have been carried out on the interactions between the rudders. Considerably more work will need to be done to determine proper interaction

factors among the hull, the propeller, and the rudder for manoeuvring simulations. Additionally, a large effective aspect ratio is desired for high effectiveness and efficiency.

Rudder performances in ship manoeuvrability, fuel consumption, and cavitation are the principle criteria to evaluate a rudder design. In general, spade rudders with efficient profiles are suggested for seagoing vessels, which sail long distance and have assistance when hard manoeuvres are needed. For inland vessels which sail independently, multiple spade rudders with high-lift profiles are recommended as they are highly effective and structurally strong. Further research is proposed on high-lift rudder profiles, multiple-rudder configurations, and interactions among the hull, the propeller, and the rudder.

Acknowledgements

The first author Jialun Liu is supported by the China Scholarship Council under Grant 201206950025. The authors would like to thank Agnieta Jansen, Elmer Brocken, Francis Mobbs, and Meno Sonnerma for their work on the tests of an inland vessel.

References

Abbott IH, Von Doenhoff AE. 1959. Theory of Wing Sections: Including a Summary of Airfoil Data. 1st ed. Dover Publications.

Ahn K, Choi GH, Son DI, Rhee KP. 2012. Hydrodynamic characteristics of X-Twisted rudder for large container carriers. International Journal of Naval Architecture and Ocean Engineering. 4(3):322–334.

Alte R, Baur MV. 1986. Propulsion Handbuch der Werften (in German). Hansa. 18:132.

Badoe CE, Phillips AB, Turnock SR. 2015. Influence of drift angle on the computation of hull-propeller-rudder interaction. Ocean Engineering. 103:64–77.

Barrass B. 2004. Ship Design and Performance for Masters and Mates. 1st ed. Oxford, UK: Elsvier Butterworth-Heinemann.

Batten WMJ, Bahaj AS, Molland AF, Chaplin J. 2006. Hydrodynamics of marine current turbines. Renewable Energy. 31(2):249–256. Marine Energy.

Batten WMJ, Bahaj AS, Molland AF, Chaplin JR. 2008. The prediction of the hydrodynamic performance of marine current turbines. Renewable Energy. 33(5):1085–1096.

Baudu H. 2014. Ship Handling. 1st ed. DOKMAR Maritime Publishers BV.

Bertagnolio F, Sørensen NN, Johansen J, Fuglsang P. 2001. Wind Turbine Airfoil Catalogue. Denmark, Forskningscenter Risoe. Risoe-R: No. 1280(EN).

Bertram V. 2012. Practical Ship Hydrodynamics. 2nd ed. Elsvier Butterworth-Heinemann.

Bonci M, Viviani M, Broglia R, Dubbioso G. 2015. Method for estimating parameters of practical ship manoeuvring models based on the combination of RANSE computations and System Identification. Applied Ocean Research. 52:274–294.

Brennen CE. 1995. Cavitation and Bubble Dynamics. Ocford, UK: Cambridge University Press.

Brix J. 1993. Manoeuvring Technical Manual. Hamburg, Germany: Seehafen Verlag.

Broglia R, Dubbioso G, Durante D, Di Mascio A. 2013. Simulation of turning circle by CFD: Analysis of different propeller models and their effect on manoeuvring prediction. Applied Ocean Research. 39:1–10.

Caldas A, Meis M, Sarasquete A. 2011. Numerical analysis of rudder effects upon ducted propeller units. In: 2nd International Symposium on Marine Propulsors; Hamburg, Germany.

Carlton JS, Radosavljevic D, Whitworth S. 2009. Rudder-propeller-hull interaction: The results of some recent research, in-service problems and their solutions. In: 1st Symposium on Marine Propulsors; Trondheim, Norway.

Champlain JG. 1971. Analysis of Flapped Rudder Gap Effects Master's thesis. Cambridge, Massachusetts, USA: Massachusetts Institute of Technology.

China Classification Society. 2003. Guidelines for Inland Vessel Manoeuvrability (in Chinese). Guidance Notes GD-2003.

Clarke D, Gedling P, Hine G. 1983. Application of manoeuvring criteria in hull design using linear theory. Transactions of the Roal Institution of Naval Architect. 125:45–68.

Cleynen O. 2011. Airfoil nomenclature; [Retrieved on 30 december 2015 from https://en.wikipedia.org/wiki/Airfoil].

Coraddu A, Dubbioso G, Mauro S, Viviani M. 2013. Analysis of twin screw ships' asymmetric propeller behaviour by means of free running model tests. Ocean Engineering. 68:47 – 64.

Det Norske Veritas. 2000. Hull equipment and appendages: Stern frames, rudders and steering gears. Rules for Classification of Steel Ships. (Part 3, Chapter 3, Section 2):6–28.

Di Mascio A, Dubbioso G, Muscari R, Felli M. 2015. CFD analysis of propeller-rudder interaction. In: 25th International Ocean and Polar Engineering Conference; Kona, Big Island, Hawaii, USA. p. 946–950.

Di Mascio A, Dubbioso G, Notaro C, Viviani M. 2011. Investigation of twin-screw naval ships maneuverability behavior. Journal of Ship Research. 55(4):221–248.

Dubbioso G, Mauro S, Ortolani F. 2015. Experimental and numerical investigation of asymmetrical behaviour of rudder/propeller for twin screw Ships. In: International Conference on Marine Simulation and Ship Maneuverability (MARSIM '15); Newcastle upon Tyne, UK.

Dubbioso G, Viviani M. 2012. Aspects of twin screw ships semi-empirical maneuvering models. Ocean Engineering. 48:69–80.

Fach K, Bertram V. 2007. High-performance simulations for high-performance ships. Ships and Offshore Structures. 2(2):105–113.

Felli M, Falchi M. 2011. Propeller tip and hub vortex dynamics in the interaction with a rudder. Experiments in Fluids. 51(5):1385–1402.

Felli M, Roberto C, Guj G. 2009. Experimental analysis of the flow field around a propeller-rudder configuration. Experiments in Fluids. 46:147–164.

Fink MP, Lastinger JL. 1961. Aerodynamic Charateristics of Low-Aspect-Ratio Wings in Close Proximity to the Ground. Washington, DC, USA: Langley Research Center.

Fujii H. 1960. Experimental researches on rudder performance (1) (in Japanese). Journal of Zosen Kiokai. (107):105–111.

Fujii H, Tsuda T. 1961. Experimental researches on rudder performance (2) (in Japanese). Journal of Zosen Kiokai. (110):31–42.

Fujii H, Tsuda T. 1962. Experimental researches on rudder performance (3) (in Japanese). Journal of Zosen Kiokai. (111):51–58.

Gim OS. 2013. Assessment of flow characteristics around twin rudder with various gaps using PIV analysis in uniform flow. Ocean Engineering. 66:1–11.

Goundar JN, Rafiuddin Ahmed M, Lee YH. 2012. Numerical and experimental studies on hydrofoils for marine current turbines. Renewable Energy. 42:173–179. International Symposium on Low Carbon and Renewable Energy Technology 2010 (ISLCT 2010).

Gregory N, O'Reilly CL. 1970. Low-Speed Aerodynamic Characteristics of NACA 0012 Aerofoil Section, including the Effects of Upper-Surface Roughness Simulating Hoar Frost. London, UK: Ministry of Defence.

Greitsch L. 2008. Prognosis of rudder cavitation risk in ship operation. In: 11th Numerical Towing Tank Symposium; Brest, France.

Greitsch L, Eljardt G, Krueger S. 2009. Operating conditions aligned ship design and evaluation. In: 1st International Symposium on Marine Propulsors; Trondheim, Norway.

Hamamoto M, Enomoto T. 1997. Maneuvering performance of a ship with VecTwin rudder system. Journal of the Society of Naval Architects of Japan. (181):197–204.

Han JM, Kong DS, Song IH, Lee CS. 2001. Analysis of the cavitating flow around the horn-type rudder in the race of a propeller. In: 4th International Symposium on Cavitation; Pasadena, CA, USA.

Harris CD. 1981. Two-Dimensional Aerodynamic Characteristics of the NACA 0012 Airfoil in the Langley 8-Foot Transonic Pressure Tunnel. Hampton, Viginia, USA: Langley Research Center.

Hasegawa K, Kang D, Sano M, Nabeshima K. 2006a. Study on the maneuverability of a large vessel installed with a mariner type Super VecTwin rudder. Journal of Marine Science and Technology. 11(2):88–99.

Hasegawa K, Kang D, Sano M, Nagarajan V, Yamaguchi M. 2006b. A study on improving the course-keeping ability of a pure car carrier in windy conditions. Journal of Marine Science and Technology. 11:76–87.

Hasegawa K, Nagarajan V, Kang DH. 2006c. Performance evaluation of Schilling rudder and Mariner rudder for Pure Car Carriers (PPC) under wind condition. In: International Conference on Marine Simulation and Ship Maneuverability (MARSIM '06); Terschelling, The Netherlands. p. 1–10. M5.

Hochkirch K, Bertram V. 2010. Engineering options for more fuel efficient ships. In: 1st International Symposium on Fishing Vessel Energy Efficiency; Vigo, Spain.

Hoerner SF. 1965. Fluid-Dynamic Drag: Practical Information on Aerodynamic Drag and Hydrodynamic Resistance. 2nd ed. Published by the Author.

Hollenbach U, Friesch J. 2007. Efficient hull forms: What can be gained? In: 1st International Conference on Ship Efficiency; Hamburg, Germany.

Hollenbach U, Reinholz O. 2011. Hydrodynamic trends in optimizing propulsion. In: 2nd International Symposium on Marine Propulsors; Hamburg, Germany.

International Maritime Organization. 2011. Amendments to the Annex of the Protocol of 1997 to Amend the International Convention for the Prevention of Pollution from Ships, 1973, as Modified by the Protocol of 1978 Relating Thereto. Resolution MEPC.203(62) Adopted on 15 July 2011.

International Maritime Organization. 2012. 2012 Guidelines on the Method of Calculation of the Attained Energy Efficiency Design Index (EEDI) for New Ships. Resolution MEPC.212(63) Adopted on 2 March 2012.

Jurgens AJ. 2005. Static and dynamic effects of rudder-hull-propeller interaction on fast monohulls. In: 8th International conference on Fast Sea Transportation (FAST 2005); St. Petersburg, Russia.

Kang D, Hasegawa K. 2007. Prediction method of hydrodynamic forces acting on the hull of a blunt-body ship in the even keel condition. Journal of Marine Science and Technology. 12(1):1–14.

Kang D, Nagarajan V, Gonno Y, Uematsu Y, Hasegawa K, Shin SC. 2011. Installing single-propeller twin-rudder system with less asymmetric maneuvering motions. Ocean Engineering. 38:1184–1196.

Kerwin JE, Lewis SD, Oppenheim BW. 1974. Experiments on rudders with small flaps in free-stream and behind a propeller. Cambridge, MA, USA: Massachusetts Institution of Technology.

Kerwin JE, Mandel P, Lewis SD. 1972a. An experimental study of a series of flapped rudders. Journal of Ship Research:221–239.

Kerwin JW, Mandel P, Lewis SD. 1972b. Hydrodynamic characteristics of flapped rudders. Journal of Mechanical Engineering Science. 14(7):142–149.

Khanfir S, Hasegawa K, Lee SK, Jang TS, Lee JH, Cheon SJ. 2008. Mathematical model for maneuverability and estimation of hydrodynamic coefficients of twin-propeller twin-rudder ship. In: The Japan Society of Naval Architects and Ocean Engineers; Osaka, Japan. p. 57–60. 7K; 2008K-G4-3.

Khanfir S, Hasegawa K, Nagarajan V, Shouji K, Lee SK. 2011. Manoeuvring characteristics of twin-rudder systems: Rudder-hull interaction effect on the manoeuvrability of twin-rudder ships. Journal of Marine Science and Technology. 2011(16):472–490.

Khanfir S, Nagarajan V, Hasegawa K, Lee SK. 2009. Estimation of mathematical model and its coefficients of ship manoeuvrability for a twin-propeller twin-rudder ship. In: International Conference on Marine Simulation and Ship Maneuverability (MARSIM '09); Panama City, Panama.

p. 159–166. vol. 8.

Kijima K, Katsuno T, Nakiri Y, Furukawa Y. 1990. On the manoeuvring performance of a ship with the parameter of loading condition. Journal of the Society of Naval Architects of Japan. (168):141–148.

Kim HJ, Kim SH, Oh JK, Seo DW. 2012. A proposal on standard rudder device design procedure by investigation of rudder design process at major Korean shipyards. Journal of Marine Science and Technology (Taiwan). 20(4):450–458.

Kim JH, Choi JE, Choi BJ, Chung SH. 2014. Twisted rudder for reducing fuel-oil consumption. International Journal of Naval Architecture and Ocean Engineering. 6(3):715–722.

Kim YG, Kim SY, Kim HT, Lee SW, Yu BS. 2007. Prediction of the maneuverability of a large container ship with twin propellers and twin rudders. Journal of Marine Science and Technology. 12(3):130–138.

Koç ST, Yılmaz S, Erdem D, Kavsaoğlu MŞ. 2011. Experimental Investigation of a Ducted Propeller. In: Proceedings of the 4th European Conference for Aerospace Sciences.

Kracht AM. 1989. Rudder in the slipstream of a propeller. In: Symposium on Ship Resistance and Powering Performance; Shanghai, China. p. 261–270.

Ladson CL. 1988. Effects of Independent Variation of Mach and Reynolds Numbers on the Low-Speed Aerodynamic Characteristics of the NACA 0012 Airfoil Section. Hampton, Viginia, USA: Langley Research Center.

Ladson CL, Hill AS, Sproles D. 1996. Computer Program To Obtain Ordinates for NACA Airfoils. NASA Technical Memorandum 4741 Hampton, Virginia, USA: National Aeronautics and Space Administration, Langley Research Center.

Laurens JM. 2003. Unsteady hydrodynamic behaviour of a rudder operating in the propeller slipstream. Ship Technology Research. 50(3):141–148.

Lee H, Kinnas SA, Gu H, Natarajan S. 2003. Numerical modeling of rudder sheet cavitation including propeller/rudder interaction and the effects of a tunnel. In: 5th International Symposium on Cavitation; Osaka, Japan. CAV03-GS-12-005.

Lee S, Rhee KP, Choi JW. 2011. Design of the roll stabilization controller using fin stabilizers and pod propellers. Applied Ocean Research. 33(4):229–239.

Lee SK, Fujino M. 2003. Assessment of a mathematical model for the manoeuvring motion of a twin-propeller twin-rudder ship. International Shipbuilding Progressh. 50(1-2):109–123.

Lehmann D. 2007. Improved propulsion with tuned rudder systems. In: 1st International Conference on Ship Efficiency; Hamburg, Germany.

Lehmann D. 2012. Station keeping with High-Performance Rudders. In: Dynamic Positioning Conference.

Liu J, Hekkenberg R. 2015. Hydrodynamic characteristics of twin-rudders at small attack angles. In: 12th International Marine Design Conference (IMDC); Tokyo, Japan. p. 177–188.

Liu J, Hekkenberg R. 2016. Suitable mesh properties for RANS analyses of aerofoils: A case study of ship rudders. Manuscript sumbitted for publication.

Liu J, Quadvlieg F, Hekkenberg R. 2015. Impacts of rudder profiles on ship manoeuvrability. In: International Conference on Marine Simulation and Ship Maneuverability (MARSIM '15); Newcastle upon Tyne, UK.

Liu J, Quadvlieg F, Hekkenberg R. 2016. Impacts of rudder profiles on manoeuvring performance of ships. Manuscript sumbitted for publication.

Loftin LK, Smith HA. 1949. Aerodynamic Characteristics of 15 NACA Airfoil Sections at Seven Reynolds Numbers from 0.7×10^6 to 9.0×10^6. Washington, USA: National Advisory Committee for Aeronautics.

Lübke L. 2009. Investigation of a semi-balanced rudder. Ship Technology Research. 56(2):69–86.

Mandel P. 1967. Ship Maneuvering and Control Phd's thesis. Hoboken, NJ, USA: Stevens Institute of Technology.

Mccroskey WJ. 1987. A Critical Assessment of Wind Tunnel Results for the NACA 0012 Airfoil. Moffett Field, CA, USA: National Aeronautics and Space Administration.

Mewis F, Klug H. 2004. The challenge of very large container ships: A hydrodynamic view. In: 9th Symposium on Practical Design of Ships and Other Floating Structures; Luebeck Travemuende, Germany. p. 173–181.

Minchev A, Schmidt M, Schnack S. 2013. Contemporary bulk carrier design to meet IMO EEDI Requirements. In: 3rd International Symposium on Marine Propulsors; Launceston, Tasmania. p. 283–291.

Molland AF. 1977. The Free-Stream Characteristics of a Semi-Balanced Ship Skeg-Rudder. Southampton, UK: University of Southampton. Ship Science Reports, 3/77.

Molland AF. 1978. Further Free-Stream Characteristics of Semi-Balanced Ship Skeg-Rudders. Southampton, UK: University of Southampton. Ship Science Reports, 2/78.

Molland AF, Bahaj AS, Chaplin JR, Batten WMJ. 2004. Measurements and predictions of forces, pressures and cavitation on 2-D sections suitable for marine current turbines. Proceedings of the Institution of Mechanical Engineers, Part M: Journal of Engineering for the Maritime Environmen. 218(2):127–138.

Molland AF, Turnock SR. 1991. Wind Tunnel Investigation of the Influence of Propeller Loading on Ship Rudder Performance. Ship Science Report No. 46 Southampton, UK: University of Southampton.

Molland AF, Turnock SR. 1992. Further Wind Tunnel Investigation of the Influence of Propeller Loading on Ship Rudder Performance. Southampton, UK: University of Southampton.

Molland AF, Turnock SR. 1993a. Wind Tunnel Investigation of the Influence of Propeller Loading on a Semi-Balanced Skeg Rudder. Southampton, UK: University of Southampton.

Molland AF, Turnock SR. 1993b. Wind Tunnel Tests on the Influence of Propeller Loading on Ship Rudder Performance: Four Quadrant Operation, Low and Zero Speed Operation. Southampton, UK: University of Southampton.

Molland AF, Turnock SR. 1995a. Some effects of rudder-propeller-hull arrangements on manoeuvring and propulsion. In: 6th International Symposium on Practical Design of Ships and Mobile Units; Korea. p. 333–345. vol. 1.

Molland AF, Turnock SR. 1995b. Wind Tunnel Tests on the Effect of a Ship Hull on Rudder-Propeller Performance at Different Angles of Drift. Southampton, UK: University of Southampton.

Molland AF, Turnock SR. 2002. Flow straightening effects on a ship rudder due to upstream propeller and hull. International Shipbuilding Progress. 49(3):195–214.

Molland AF, Turnock SR. 2007. Marine Rudders and Control Surfaces: Principles, Data, Design and Applications. 1st ed. Elsevier.

Molland AF, Turnock SR, Smithwick JET. 1995. Wind Tunnel Tests on the Influence of Propeller Loading and the Effect of a Ship Hull on Skeg-Rudder Performance. Southampton, UK: University of Southampton.

Motoki A, Kunihide Ohashi, Nobuaki S. 2015. Effects of rudder horn and propelelr hub vortex for CFD manoeuvring simulations. In: International Conference on Marine Simulation and Ship Maneuverability (MARSIM '15); Newcastle upon Tyne, UK.

Nagarajan V, Kang DH, Hasegawa K, Nabeshima K. 2008. Comparison of the mariner Schilling rudder and the mariner rudder for VLCCs in strong winds. Journal of Marine Science and Technology. 13:24–39.

Nagarajan V, Kang DH, Hasegawa K, Nabeshima K, Arii T. 2009. A proposal for propulsion performance prediction of a single-propeller twin-rudder ship. Journal of Marine Science and Technology. 14:296–309.

Natarajan S. 2003. Computational Modeling of Rudder Cavitation and Propeller/Rudder Interaction Master's thesis. Austin, TX, USA: The University of Texas.

Nienhuis U. 1987. Passieve Manoeuvreerhulpmiddelen: Open Water Proeven met Roer (in Dutch). Wageningen, The Netherlands: Maritime Research Institute Netherlands (MARIN).

Olson CR. 1955. Effects of Various Linkage Ratios on the Free-Stream Hydrodynamic Characteristics of an All-Movable Flapped Rudder. Washington, DC, USA: David Taylor Model Basin.

Oppenheim BW. 1974. A Theoretical and Experimental Investigation of the Performance of Flapped Rudders Master's thesis. Massachusetts Institute of Technology.

Pecoraro A, Di Felice F, Felli M, Salvatore F, Viviani M. 2015. An improved wake description by higher order velocity statistical moments for

single screw vessel. Ocean Engineering. 108:181–190.

Pelletier A, Mueller TJ. 2000. Low Reynolds Number aerodynamics of low-aspect-ratio, thin/flat/cambered-plate wings. Journal of Aircraft. 37(5):825–832.

Perez T. 2005. Ship Motion Control: Course Keeping and Roll Stabilisation Using Rudder and Fins. Springer.

Phillips AB, Turnock SR, Furlong M. 2010. Accurate capture of rudder-propeller interaction using a coupled blade element momentum-RANS approach. Ship Technology Research. 57(2):128–139.

Quadvlieg FHHA. 2013. Mathematical models for the prediction of manoeuvres of inland ships: Does the ship fit in the river? In: Rigo P, Wolters M, editors. Smart Rivers 2013; Liège, Belgium/Maastricht, The Netherlands. PIANC; p. 187.1–187.9.

Ram BRR, Surendran S, Lee SK. 2015. Computer and experimental simulations on the fin effect on ship resistance. Ships and Offshore Structures. 10(2):121–131.

Reichel M. 2009. Influence of rudder location on propulsive characteristics of a single screw container ship. In: 1st International Symposium on Marine Propulsors; Trondheim, Norway. p. 1–6.

Ren R, Zou Z, Wang X. 2014. A two-time scale control law based on singular perturbations used in rudder roll stabilization of ships. Ocean Engineering. 88:488–498.

Rhee SH, Lee C, Lee HB, Oh J. 2010. Rudder gap cavitation: Fundamental understanding and its suppression devices. International Journal of Heat and Fluid Flow. 31(4):640–650.

Sarasquete A, Collazo AC, Coache S, Meis M, Ruiz V. 2012. Increased energy efficiency of the fishing fleet due to improved hydrodynamic performance. In: 2nd International Symposium on Fishing Vessel Energy Efficiency; Vigo, Spain.

Sathaye SS. 2004. Lift Distributions on Low Aspect Ratio Wings at Low Reynolds Numbers Master's thesis. Worcester Polytechnic Institute.

Schilling K. 1963. Rudder Control Arrangement; [United stated patent office, 3,101,693].

Schilling K, Rathert H. 1978. Dual Rudder Assembly; [United stated patent office, 4,085,694].

Schneekluth H, Bertram V. 1998. Ship Design for Efficiency and Economy. 2nd ed. Elsevier Butterworth-Heinemann.

Sharif MT, Roberts GN, Sutton R. 1995. Sea-trial experimental results of fin/rudder roll stabilisation. Control Engineering Practice. 3(5):703–708.

Sharif MT, Roberts GN, Sutton R. 1996. Final experimental results of full scale fin/rudder roll stabilisation sea trials. Control Engineering Practice. 4(3):377–384.

Shen YT, Jiang CW, Remmers KD. 1997a. A twisted rudder for reduced cavitation. Journal of Ship Research. 41(4):260–272.

Shen YT, Remmers KD, Jiang CW. 1997b. Effects of ship hull and propeller on rudder cavitation. Journal of Ship Research. 41(3):172–180.

Shiba H. 1960. Model experiments about the maneuverability of turning of ships. In: First Symposium on Ship Maneuverability; Washington, DC, USA. David Taylor Model Basin; David Taylor Model Basin.

Simonsen CD. 2000. Rudder, Propeller and Hull interaction by RANS Phd's thesis. Technical University of Denmark.

Söding H. 1982. Prediction of ship steering capabilities. Schiffstechnik. 29(1):3–29.

Stierman EJ. 1989a. The influence of the rudder on the propulsive performance of ships, Part I. International Shipbuilding Progress. 36(407):303–334.

Stierman EJ. 1989b. The influence of the rudder on the propulsive performance of ships, Part II. International Shipbuilding Progress. 36(407):303–334.

Stuck A, Turnock S, Bressloff N. 2004. An Evaluation of the RANS Method for the Prediction of Steady Ship Rudder Performance Compared to Wind Tunnel Measurements. Southampton, UK: University of Southampton.

Surendran S, Kiran V. 2006. Technical note Studies on the feasibilities of control of ship roll using fins. Ships and Offshore Structures. 1(4):357–365.

Surendran S, Kiran V. 2007. Control of ship roll motion by active fins using fuzzy logic. Ships and Offshore Structures. 2(1):11–20.

Tabaczek T. 2010. Numerical simulation of planar motion of a twin-screw inland waterway vessel in shallow water. In: 18th International Confer-

ence on Hydrodynamics in Ship Design, Safety and Operation; Gdansk, Poland. p. 37–50.

Takekoshi Y, Kawamura T, Yamaguchi H, Maeda M, Ishii N, Kimura K, Taketani T, Fujii A. 2005. Study on the design of propeller blade sections using the optimization algorithm. Journal of Marine Science and Technology. 10(2):70–81.

Thieme H. 1962. Zur formgebung von shiffsrudern. Jahrbuch der Schiffbautechnische Gesellschaft. 56:381–426.

Thieme H. 1965. Design of Ship Rudders (Zur Formgebung von Shiffsrudern, originally published in German 1962, translated by E. N. Labouvie). Washington, DC, USA: Shipbuilding Institute, University of Hamburg.

Timmer WA. 2010. Aerodynamic characteristics of wind turbine blade airfoils at high angles-of-attack. In: 3rd EWEA Conference-Torque 2010: The Science of making Torque from Wind; Heraklion, Crete, Greece. European Wind Energy Association.

Torres GE, Mueller TJ. 2004. Low-aspect-ratio wing aerodynamics at low Reynolds Numbers. AIAA Journal. 42(5):865–878.

Turnock SR. 1990. A Test Rig for the Investigation of Ship Propeller/Rudder Interactions. Ship Science Report No. 45 Southampton, UK: University of Southampton.

Turnock SR. 1993. Prediction of Ship Rudder-Propeller Interaction Using Parallel Computations and Wind Tunnel Measurements [dissertation]. University of Southampton.

Turnock SR, Wright AM. 2000. Directly coupled fluid structural model of a ship rudder behind a propeller. Marine Structures. 13(1):53–72.

Ueno M, Tsukada Y. 2015. Rudder effectiveness and speed correction for scale model ship testing. Ocean Engineering. 109:495–506.

Ueno M, Tsukada Y, Kitagawa Y. 2014. Rudder effectiveness correction for scale model ship testing. Ocean Engineering. 92:267–284.

Van Amerongen J. 1991. Ship rudder roll stabilization. In: Papageorgiou M, editor. Concise encyclopedia of traffic & transportation systems. Amsterdam, The Netherlands: Pergamon; p. 448–454.

Van Amerongen J, Van Der Klugt PGM, Van Nauta Lemke HR. 1990. Rudder roll stabilization for ships. Automatica. 26(4):679–690.

Van Beek T. 2004. Technology guidelines for efficient design and operation of ship propulsors. Marine News, Wärtsillä Propulsion, Netherlands BV. 1:14–19.

Van Nguyen T, Ikeda Y. 2013. Hydrodynamic characteristic of rudder sections with high lift force. Journal of the Japan Society of Naval Architects and Ocean Engineers. (19):403–406.

Van Nguyen T, Ikeda Y. 2014a. Development of fishtail rudder sections with higher maximum lift coefficients. In: 24th International Ocean and Polar Engineering Conference; Busan, Korea. p. 940–947.

Van Nguyen T, Ikeda Y. 2014b. Hydrodynamic characteristic of rudder sections with high lift force (Part 2): The wedge tail shapes. Journal of the Japan Society of Naval Architects and Ocean Engineers. (18):171–174.

Whicker LF, Fehlner LF. 1958. Free-Stream Characteristics of a Family of Low-Aspect-Ratio, All-Movable Control Surfaces for Application to Ship Design. Washington, DC, USA: David Taylor Model Basin.

Yang H, Lee J, Kim K. 2015. Numerical and Experimental study on the rudder force of a twisted rudder. In: International Conference on Marine Simulation and Ship Maneuverability (MARSIM '15); Newcastle upon Tyne, UK.

Yasukawa H, Yoshimura Y. 2014. Introduction of MMG standard method for ship maneuvering predictions. Journal of Marine Science and Technology. 20(1):37–52.

Yılmaz S, Erdem D, Kavsaoğlu MŞ. 2013. Effects of duct shape on a ducted propeller performance. In: 51st AIAA Aerospace Sciences Meeting including the New Horizons Forum and Aerospace Exposition; Grapevine, Texas. p. 1–11.

Yoo WJ, Yoo BY, Rhee KP. 2006. An experimental study on the maneuvering characteristics of a twin propeller/twin rudder ship during berthing and unberthing. Ships and Offshore Structures. 1(3):191–198.

Yoshimura Y, Sakurai H. 1989. Mathematical model for the manoeuvring ship motion in shallow water (3rd report): Manoeuvrability of a twin-propeller twin-rudder ship. Journal of the Kansai Society of Naval Architects, Japan. 211:115–126.